

Cybersecurity of Quantum Key Distribution Implementations

Ittay Alfassi¹, Ran Gelles², Rotem Liss³, and Tal Mor¹

¹Computer Science Department, Technion—Israel Institute of Technology, Haifa, Israel,
{ittay.al,talmo}@cs.technion.ac.il

²Faculty of Engineering, Bar-Ilan University, Ramat Gan, Israel, ran.gelles@biu.ac.il

³ICFO—Institut de Ciències Fòniques, The Barcelona Institute of Science and Technology, Castelldefels
 (Barcelona), Spain, rotem.liss@icfo.eu

Abstract

Practical implementations of Quantum Key Distribution (QKD) often deviate from the theoretical protocols, exposing the implementations to various attacks even when the underlying (ideal) protocol is proven secure. We present new analysis tools and methodologies for *quantum cybersecurity*, adapting the concepts of vulnerabilities, attack surfaces, and exploits from classical cybersecurity to QKD implementation attacks. We present three additional concepts, derived from the connection between classical and quantum cybersecurity: “Quantum Fuzzing”, which is the first tool for black-box vulnerability research on QKD implementations; “Reversed-Space Attacks”, which are a generic exploit method using the attack surface of imperfect receivers; and a concrete quantum-mechanical definition of “Quantum Side-Channel Attacks”, meaningfully distinguishing them from other types of attacks. Using our tools, we analyze multiple existing QKD attacks and show that the “Bright Illumination” attack could have been fully constructed even with minimal knowledge of the device implementation. This work begins to bridge the gap between current analysis methods for experimental attacks on QKD implementations and the decades-long research in the field of classical cybersecurity, improving the practical security of QKD products and enhancing their usefulness in real-world systems.

1 Introduction

Quantum Key Distribution (QKD) [1, 2, 3, 4, 5] allows two parties to generate a secret shared key whose unconditional security is guaranteed by the principles of quantum mechanics. In recent decades, many security proofs for QKD have been devised (e.g., [6, 7, 8, 9, 10, 11]), proving security under specific theoretical assumptions.

QKD schemes have not only been described theoretically, but also implemented in practice, including in laboratory experiments and commercial products [12, 13, 14, 5, 15].

Unfortunately, those real-world implementations of QKD inevitably deviate from the idealized models assumed in security proofs, leading to possibly exploitable loopholes. As a simple example, while most QKD schemes are based on qubits, they are implemented by sending and receiving photons, which actually reside in a quantum space of higher dimension. Such mismatches between theoretical models and practical implementations of QKD have given rise to various attacks that effectively compromise the security of the secret key [16, 17, 18, 19, 20, 21, 22, 23, 24]; these attacks highlight the need for a deeper understanding of security in *practical* QKD systems and better ways to analyze their security.

In contrast to the analysis of QKD imperfections, the security analysis and certification of practical implementations of communication systems have been thoroughly researched in the classical field of cybersecurity, resulting in well-established methods for such analyses [25, 26]. The first step in such an analysis is to review the interfaces of the system with potential adversaries, interfaces named *the attack surface*. The next step (called “vulnerability research”)

is to search for *vulnerabilities*, which are unwanted behaviors of the system, some related to the protocol and some to the environment, the latter called *side channels*. The final step is to build an *exploit*: an attack that uses the detected vulnerabilities.

The purpose of this paper is to build an analogous set of tools for *quantum cybersecurity*, bringing insights from classical cybersecurity into the world of QKD systems. We begin by defining equivalents of concepts and tools from classical cybersecurity, including vulnerabilities, attack surfaces, and exploits (Section 3). We then show how to decompose QKD implementation attacks into those components and analyze each component separately, enabling QKD system designers to systematically discover and prevent possible attacks.

Then, we define the first vulnerability research method for QKD implementations, which we name *Quantum Fuzzing* (see Section 4). This method is analogous to the notion of classical fuzzing, which “experiments” with unusual inputs to an implementation in order to expose vulnerabilities. Adapting this concept to the quantum world, we enable QKD system designers and attackers to discover vulnerabilities in a QKD system, even if their knowledge of its inner workings is limited.

We next define a general family of attacks named *Reversed-Space Attacks* (Section 5), which is a generic exploit method for discovered vulnerabilities. This method, initially introduced in the preliminary work [27, 28], begins by finding the *reversed space* of the QKD implementation, which is derived by reversing states that are measured by the QKD device “back in time”. This space is essentially the receiving party’s *attack surface*, because it exactly describes the quantum space affecting their measurements. Then, the method uses the reversed space to construct a successful attack (see Appendix B for a detailed example). We note that an additional important example of a reversed-space attack is the “fixed-apparatus attack”, which appeared in [24].

In contrast to attacks that only rely on the transmitted and received quantum states, there are also attacks that utilize unmeasured side channels; such attacks are named “side-channel attacks”. Side-channel attacks on quantum devices have appeared in the literature [20, 21, 29, 30]. However, previous definitions were too general, because *all* attacks on QKD systems rely on physical faults. We thus give a new and meaningful definition of *Quantum Side-Channel Attacks* (see Section 6).

To demonstrate how the methods we developed can help devise and analyze attacks on practical QKD implementations, we show that the *Bright Illumination attack* [31, 21, 32] is, in fact, a delicately crafted exploitation of the tools defined in this paper (see Section 7). Finally, we use our tools to classify well-known attacks on practical QKD implementations (see Section 8).

Initial versions of (subsets of) the results presented in this paper previously appeared in [27] (see also extended results in [28]) and [32].

1.1 Other Related Work

Our work focuses on QKD scheme implementations using *photons*. This is not a limitation, since all commercial implementations and almost all experimental implementations of QKD are photon-based [12, 13, 14, 5, 15, 33, 34, 35, 36, 37].

Many attacks on QKD implementations have appeared in the literature (see, e.g., [16, 17, 18, 21, 22, 23, 24]; see Appendix G for more details). Previous works have also classified certain similar attacks together as “attack families”, which are sets of attacks that share common principles; two examples include the “faked states” attack family [19, 20] and the “Detector Efficiency Mismatch” attack family [38].

A thorough survey of attacks on QKD implementations was given in [30]. In addition, the term “vulnerabilities” in reference to QKD imperfections was also used in the review [39].

Finally, in this paper, we use classical cybersecurity terminology that has been commonplace in the last few decades; see [25] for an educational handbook and the NIST SP 800 documents [26]

for an international cybersecurity standard. Both provide documentation of this terminology, as well as a broad introduction to classical cybersecurity as a whole.

2 Preliminaries

2.1 The (Ideal) BB84 Protocol

In the BB84 QKD protocol [1], Alice sends to Bob N qubits, each of them randomly chosen from the set of quantum states $\{|0\rangle, |1\rangle, |+\rangle \triangleq \frac{|0\rangle+|1\rangle}{\sqrt{2}}, |-\rangle \triangleq \frac{|0\rangle-|1\rangle}{\sqrt{2}}\}$, and Bob measures each of them either in the computational basis $\{|0\rangle, |1\rangle\}$ or in the Hadamard basis $\{|+\rangle, |-\rangle\}$, chosen randomly. Thereafter, Alice and Bob post-process the results by using an authenticated classical channel. If Alice and Bob used matching bases, they now share a bit (unless there is some noise or eavesdropping); if they use mismatching bases, Bob’s results are random. Alice and Bob reveal their basis choices and discard the bits for which they used mismatching bases. After that, they publicly reveal a random subset of their bits in order to estimate the error rate (then discarding those exposed test bits), aborting the protocol if the error rate is too high; and they perform error correction and privacy amplification processes, obtaining a completely secret, identical final key.

2.2 Realistic QKD Implementations and Fock Space Notation

While the ideal BB84 (and other QKD protocols) communicates using abstract qubits, any experimental implementation must rely on physical, easy-to-transfer quantum carriers, which encode qubits. In most existing implementations, *photons* serve as such carriers. A very well-known example (e.g., [12]) is the BB84 implementation that uses two polarization modes to encode a qubit: namely, the polarizations \leftrightarrow and \updownarrow signify $|0\rangle$ and $|1\rangle$ respectively, and the orthogonal diagonal photon polarizations encode $|+\rangle$ and $|-\rangle$.

Fock States. To accurately describe photonic quantum systems, one can use Fock Space notation (or simply, Fock states). Photons are physical systems with many quantum degrees of freedom, called *modes*, that describe different characteristics of the photons such as their polarization, location, etc.

Specifically, the Fock state $|m\rangle^F$ represents m identical photons in a single photonic mode.¹ If the system uses photons with different characteristics, they are represented by different modes. In particular, the state $|m_1\rangle^F \otimes |m_0\rangle^F \equiv |m_1\rangle^F |m_0\rangle^F \equiv |m_1, m_0\rangle^F$ describes m_0 photons in the first mode and m_1 photons in the second mode. This can be extended to any number of modes and photons in each mode.

Using this notation, the above polarization-based implementation can be expressed using two modes, i.e., one mode to signify photons in the \leftrightarrow polarization and another mode for \updownarrow . The state $|0\rangle = |0, 1\rangle^F$ describes a single photon with horizontal polarization, and $|1\rangle = |1, 0\rangle^F$ describes a single photon with vertical polarization. Similarly, in implementations that encode a qubit onto the *time* at which a photon arrives, we can define two distinct time bins: t_0 and t_1 . In this case, $|0\rangle = |0, 1\rangle_{t_1, t_0}^F$ is a photon arriving at the first time-bin, and $|1\rangle = |1, 0\rangle_{t_1, t_0}^F$ is a single photon arriving at the second time-bin. We will use $|V\rangle = |0, 0\rangle^F$ to denote the *vacuum* state — a state with zero photons in all modes. Note that since photons are indistinguishable and have integer spin, the state remains identical when photons “switch places”, and there is no upper bound on the number of photons in each mode.

Realistic Measurement of Photons. Theoretically, measurement of the Fock state $|m\rangle^F$ can yield the number of photons occupying the mode — that is, the number m . This can be

¹We use the notation $|\cdot\rangle^F$ to indicate use of the occupancy number basis.

extended to an ideal measurement of the k -mode Fock state $|m_{k-1}, \dots, m_1, m_0\rangle^F$ which yields the numbers m_0 to m_{k-1} . However, as shown in the following sections, realistic devices are typically unable to count the exact number of photons.

In addition, one can measure other specific properties of the state using linear optical tools, such as beam splitters, phase shifters, and mirrors (see [40]). Details on the applications of these tools on photonic quantum states can be found in Appendix A.

3 Classical and Quantum Cybersecurity

The security of classical computing systems, including the structure of potential weaknesses and methods for their analysis, has been extensively researched in the field of classical cybersecurity. In this section we explain the concepts and methodology used for analyzing computing systems via classical cybersecurity, and we explain how they can be utilized and applied to the world of QKD implementations.

3.1 Classical Cybersecurity

The concepts of classical cybersecurity are best described using an example: we consider a blog website running on a server. A security researcher can analyze the security of that blog using the following method:

1. **Examining the Attack Surface.** The first step in analyzing a system's security is to examine the various interfaces through which an attacker could gain access. In a standard website-based blog, an attacker can target any interface normally available to all blog readers. For example, a reader can typically post a comment by sending a "post comment" request. Sometimes, there are additional available interfaces. For instance, there might be a way to send and receive files from the blog-hosting server (also known as an FTP interface), or even access the blog administrator's interface. These interfaces may be blocked to external connections, protected by passwords, or left completely open. Other potential interfaces, such as physical access to the server (for example, plugging in an infected USB drive), are not available to an attacker outside the premises, but could be available to an internal attacker, such as a malicious employee.

The collection of interfaces accessible to an attacker is called the *attack surface* of the system.

Definition 1. *An attack surface is "the set of points on the boundary of a system, a system element, or an environment where an attacker can try to enter, cause an effect on, or extract data from". [26]*

Note that this is a broad definition, which means that when analyzing a system's attack surface, one must take into account all possible interfaces an attacker has with the system and all potential effects those interfaces can have on it.

2. **Detecting and Analyzing Vulnerabilities.** Once our security researcher examines the attack surface of the blog, they can try finding *loopholes*, i.e., flaws in the implementation of the blog, that may be exploited in order to gain unauthorized access to some functionality or resource of the system. Such imperfections are called *vulnerabilities*.

Definition 2. *A vulnerability is "a flaw in a system's security that can lead to an attacker utilizing the system in a manner other than that which the designer intended". [25]*

Naturally, a security researcher should focus on vulnerabilities that are accessible through the system’s attack surface. Other vulnerabilities, even if they exist and could enable harmful attacks, are irrelevant to developing an exploit by the considered attacker.

An example of a well-known vulnerability is a “Buffer Overflow” (BOF) (see, e.g., [41]), where a program writes data to an array of bytes (a buffer) that is shorter than the data length. This causes the data to overflow from the confines of the dedicated buffer to the next memory cells, affecting other data in the computer’s memory. In the context of our blog website, such a vulnerability may occur in the code handling the “post comment” request if a user can send, for example, an arbitrarily long email address while the server allocates a fixed-size buffer to store it.

The vulnerabilities mentioned above are based on direct interaction of the user (or the attacker) with the system. In contrast, there are vulnerabilities that rely on indirect interaction of the attacker with the system, extending beyond standard inputs and outputs. Attacks based on this different type of vulnerability are known as *side-channel attacks*. As a toy example, consider the case where the blog verifies a user’s password by comparing it one character at a time to the stored password (instead of storing a hash of the password), and the server does not limit the amount of login attempts. An attacker could measure the blog’s response time to infer how many characters were matched correctly.

3. **Developing Exploits.** The mere existence of a vulnerability, even if it causes some undesired behavior, is not sufficient by itself to compromise a system’s security. To do so, the vulnerability must be triggered as part of a well-planned *attack*, which can produce the desired effect on the target system. For example, if an attacker finds out that the blog has a Buffer Overflow vulnerability when processing an email input, they can submit a well-crafted email-like input whose overflowing part would make the blog’s server run some malicious code.

An attack that utilizes a vulnerability in order to gain unauthorized access to a system or its data, or to maliciously affect them, is called an *exploit* (as a noun).

Definition 3. *An exploit is a “tool, set of instructions, or code that is used to take advantage of a vulnerability”. [25].*

The above concepts are highly beneficial for analyzing attacks on computing systems because of their ability to *decompose attacks into separate stages and components*. Once each component is considered separately, researchers can better understand how this component behaves, find more instances of it, and build tools to defend against it. For example, researching vulnerabilities has given rise to definitions of common types of vulnerabilities [41], methods for discovering vulnerabilities in code [42], and coding practices that minimize vulnerabilities [43]. Researching attack surfaces has given rise to attack surface characterization methods [44], as well as tools for minimizing attack surfaces (such as firewalls). Researching the concept of exploits has given rise to generic exploit methods [45], as well as defense mechanisms that prevent exploits [46, 47].

3.2 Cybersecurity of QKD systems

We can now analyze the security of QKD systems through the lens of the (classical) cybersecurity analysis framework depicted above, extending the classical framework to QKD systems. This allows us to decompose complete attacks into their constituent components and analyze each one in detail, as is standard practice in classical cybersecurity.

3.2.1 Vulnerabilities

Vulnerabilities in QKD systems are certain “imperfections” and “weaknesses” that occur in practical implementations when they deviate from the model defined by the theoretical protocol.

We will now give examples of such imperfections, both in Alice’s state preparation devices and in Bob’s measurement devices.

Vulnerabilities in Alice’s Preparation Devices: Photon-Number Splitting A common form of vulnerability in Alice’s devices is that Alice sometimes sends different states than those she intended. A well-known example of such a vulnerability can be seen in the *Photon-Number Splitting* (PNS) attack [16, 48] (which showed all QKD experiments done until around year 2000 to be insecure). The PNS vulnerability is based on a fault in Alice’s transmitter that sometimes sends *two-photon pulses* (instead of a single photon) in one of the four allowed configurations.

Eve can build an exploit based on this vulnerability by distinguishing the two-photon pulses from the single-photon pulses, keeping one photon for herself, then measuring it once the classical bases are revealed.

Vulnerabilities in Bob’s Detectors A common vulnerability in Bob’s detectors is that they measure a Hilbert space larger than an ideal qubit. This enlargement can arise either from flaws in the physical components or from deliberate expansions of the measurement space by Bob’s devices. We now present two examples of such vulnerabilities caused by physical imperfections.

Example 1: Photon Number Resolution Suppose Alice sends a perfect qubit encoded into the polarization of a single photon, and yet Bob uses a detector that cannot distinguish a single photon from a pair of photons (commonly called a “threshold detector”). Thus, while Alice only sends states from the Hilbert space $\text{span}\{|1, 0\rangle^F, |0, 1\rangle^F\}$, if the state $|2, 0\rangle^F$ arrives at Bob’s detector, the detector cannot distinguish it from the state $|1, 0\rangle^F$. Thus, Eve can attack a larger space than is possible in the ideal case.²

Example 2: Detection Timing Suppose Alice sends a perfect qubit encoded to the polarization of a single photon, which arrives at a specific time t , and yet Bob cannot exactly distinguish *when* a photon arrives. Namely, for some delay $\delta > 0$, he treats late photons that arrive at $t + \delta$ the same as photons that arrive correctly at time t . Modeling this example using Fock states, with four modes describing “horizontal at t ”, “vertical at t ”, “horizontal at $t + \delta$ ” and “vertical at $t + \delta$ ”, Alice’s qubit is encoded using the span of $\{|1, 0, 0, 0\rangle^F, |0, 1, 0, 0\rangle^F\}$, but Bob interprets $|0, 0, 1, 0\rangle^F$ the same as $|1, 0, 0, 0\rangle^F$ and interprets $|0, 0, 0, 1\rangle^F$ the same as $|0, 1, 0, 0\rangle^F$.

Examples of Vulnerability Classes in QKD Taking inspiration from the examples above, we define two classes of vulnerabilities in Bob’s system that will serve us throughout the paper.

The first class of vulnerabilities describes a deviation from the theoretical protocol that almost always occurs: Bob’s detectors measure more than the space on which the protocol states are encoded. Thus, the space Bob measures is larger than it has to be.

Definition 4. A Measurement Space Vulnerability occurs when Bob’s measured space differs from the space defined in the theoretical protocol.

An example of a Measurement Space Vulnerability is a detector that measures pulses at time t and at time $t + \delta$, when it should only measure at time t , as seen in Example 2 above.

A Measurement Space Vulnerability is often not exploitable into a full attack by itself, since there is another critical element in Bob’s system: the *interpretation* of the new, unexpected states. When Bob measures a different space than he should, he might also “confuse” states that belong in the ideal space with states that do not. We now define a second class of vulnerabilities, named *Interpretation Vulnerabilities*, that describe this phenomenon.

²There are known ways to mitigate this vulnerability, such as through the squashing model [49].

Definition 5. *An Interpretation Vulnerability occurs when Bob’s interpretation of measured states as valid states differs from the theoretical protocol.*

Example 2 above also illustrates an Interpretation Vulnerability: Bob does not only measure pulses at $t + \delta$, but also interprets the time-shifted states as if they were not shifted. Thus, Example 2 can be decomposed into two parts: a Measurement Space Vulnerability, in which additional states are measured, and an Interpretation Vulnerability, in which those states are misinterpreted. This holds in general: an Interpretation Vulnerability must always be accompanied by a Measurement Space Vulnerability.

Additional interesting properties of these vulnerability classes will be discussed in the following subsections.

3.2.2 Attack Surface

The attack surface of a QKD implementation can be divided into two components. The first includes interfaces defined by state spaces the devices use. The second regards other elements in the devices that interact with the environment, and by extension, with the attacker. Let us describe these two in turn.

The state space in use. Every QKD device, be it Alice’s or Bob’s, uses a specific state space for its operation. Each state space is a component of the system’s attack surface. In Alice’s device, the state space component of the attack surface is the span of the states she transmits. For example, in the ideal BB84, Alice transmits qubits. However, implementation vulnerabilities can enlarge this space: for example, if Alice’s device suffers from the Photon Number Splitting (PNS) vulnerability, her attack surface changes from the space spanned by her attack surface becomes the space spanned by $\{|1, 0\rangle^F, |0, 1\rangle^F\}$ to the space spanned by $\{|0, 0\rangle^F, |1, 0\rangle^F, |0, 1\rangle^F, |2, 0\rangle^F, |1, 1\rangle^F, |0, 2\rangle^F\}$.

In Bob’s device, the state space component of the attack surface is the space that affects Bob’s measurement. For example, in the ideal BB84, this is again the qubit space. However, if Bob’s device suffers from the detection timing vulnerability stated in Example 2, instead of being affected by the space spanned by $\{|1, 0, 0, 0\rangle^F, |0, 1, 0, 0\rangle^F\}$, he will be affected by the span of $\{|1, 0, 0, 0\rangle^F, |0, 1, 0, 0\rangle^F, |0, 0, 1, 0\rangle^F, |0, 0, 0, 1\rangle^F\}$. The connection to Measurement Space Vulnerabilities (Definition 4) is clear: if a device suffers from a Measurement Space Vulnerability, the space it measures is different from the ideal space, which modifies the attack surface and usually enlarges it, as occurs in the above example.

Elements that interact with the environment. Every device interacts with its physical environment to a certain degree. Depending on how drastically a QKD device can be affected through the interaction with the environment, or how much internal information is exposed through it, the interaction with the environment can enable critical attacks on the QKD device. For example, consider the physical configuration of Alice’s or Bob’s device when they prepare to send or measure a state. If this configuration can somehow be probed by Eve, then it is part of the attack surface of the devices, and Eve can potentially use it for an attack [17]. Section 6 defines attacks based on this part of the attack surface as “Quantum Side-Channel Attacks” and includes a detailed explanation of the above example.

3.2.3 Exploits

Similarly to the classical-world definition, an exploit is an attack that utilizes a vulnerability in the system. In QKD implementations, such an attack is usually modeled as a single unitary transformation that Eve can apply, although in the most general case it can be modeled as a multi-stage procedure.

Since all successful attacks on QKD must be based on some imperfection in the implementation, every successful attack can be partitioned into two parts: a vulnerability (or several vulnerabilities) and an exploit that utilizes it. This decomposition of all attacks to vulnerabilities and exploits highlights, just like in classical systems, that finding a vulnerability in a QKD system is *not enough* to attack it. To carry out a successful attack, the vulnerability must be used through a matching exploit. From this we conclude that building exploits is a field of its own that requires careful consideration; in fact, even when a vulnerability (or several ones) is already known, building an exploit is a completely separate task which can be very challenging.

Generic exploit methods. A common theme in exploit research for classical cybersecurity is the idea of generic exploit methods that apply to *classes* of vulnerabilities, and not necessarily to one specific instance of a vulnerability. Assuming that a class of vulnerabilities trigger similar behavior in a system (often called a *primitive* in classical cybersecurity), one can build a generic exploit method that relies on that behavior. This idea is also commonplace in existing QKD literature discussing “attack families”.

One known example is the “faked states” attack family [19]. Attacks in this family share one common property: Eve receives the state that Alice sent, measures it, and then re-sends a state that will force a *specific* interpretation in Bob’s system. Using our new methodology, this attack family can be decomposed to a set of vulnerabilities where fake, out-of-protocol states can force a specific interpretation, and a single, generic exploit method (which is discussed below).

Another known example is the *detector efficiency mismatch* attack family [20], which is a special case of the *faked states* attack family. Attacks in this family rely on vulnerabilities where different detectors are more/less sensitive depending on some characteristic of the input states. The generic exploit of this attack family creates attacks that manipulate this characteristic, such that whenever Eve and Bob choose different bases, Bob is less likely to detect the modified signal.

Section 5 shows a novel attack family called *Reversed-Space Attacks*, which is a generic exploit method for the Measurement Space Vulnerability and Interpretation Vulnerability classes defined in Section 3.2.1 above.

Example: Faked States exploit. We now explicitly show the generic exploit that all faked states attacks are based on, in the form of unitary transformations. As stated above, all faked-states attacks are based on the same type of vulnerability: there is a state that Eve can send, which forces a specific bit and basis interpretation in Bob’s system.

In this exploit, Eve begins by choosing either the computational or the Hadamard basis (for each transmission). Then, Eve’s unitary transformation changes each basis state from her chosen basis into its “faked” counterpart, which will then force the desired bit and basis detection in Bob’s system. Eve’s unitary also stores the value of her sent faked state in her own ancilla register, which she then measures.

Let us denote a BB84 state entering Bob’s system as $|\psi\rangle_B$, and its faked counterpart as $|\psi_{\text{fake}}\rangle_B$. Let the vectors $|E_0\rangle_E^{\text{anc}}, |E_1\rangle_E^{\text{anc}}, |E_2\rangle_E^{\text{anc}}, |E_3\rangle_E^{\text{anc}}$ be four orthogonal state vectors, and let U_E^C and U_E^H be Eve’s unitary operations (depending on her basis choice).

A faked state attack on a BB84 implementation is of the form:

$$\begin{aligned} U_E^C |0\rangle_A |0\rangle_E^{\text{anc}} &= |0_{\text{fake}}\rangle_B |E_0\rangle_E^{\text{anc}}, & U_E^H |+\rangle_A |0\rangle_E^{\text{anc}} &= |+\text{fake}\rangle_B |E_2\rangle_E^{\text{anc}}, \\ U_E^C |1\rangle_A |0\rangle_E^{\text{anc}} &= |1_{\text{fake}}\rangle_B |E_1\rangle_E^{\text{anc}}, & U_E^H |-\rangle_A |0\rangle_E^{\text{anc}} &= |-\text{fake}\rangle_B |E_3\rangle_E^{\text{anc}}, \end{aligned} \quad (1)$$

This example illustrates the distinction between the specific vulnerability of Bob’s device, and the generic exploit method which can be applied to any vulnerability from the type we analyze. It thus shows the importance and usefulness of separating the process of finding vulnerabilities (commonly referred to as “vulnerability research”) from the process of devising

an exploit, whether it is a tailor-made exploit for one specific vulnerability, or a generic exploit method for a set of vulnerabilities.

4 Quantum Fuzzing: Vulnerability Research for QKD

In this section, we define “Quantum Fuzzing”, which is the first systematic vulnerability research method for QKD devices. In classical cybersecurity, vulnerability research is the process of analyzing a device’s implementation in order to detect currently unknown vulnerabilities and issues. While it is quite common for classical system designers and attackers to perform, it has yet to be applied to QKD, where, in theory, all devices are provably secure, and all adversaries are aware of all possible attacks on a device. We show that this process becomes crucial when considering practical QKD implementations and adversaries. Our method, which relies on minimal knowledge of a device’s inner workings, enables system designers to detect issues that would otherwise require expert knowledge to be identified, or worse, would only be discovered when it is too late.

4.1 Motivation: Practical Adversaries for QKD Systems

QKD protocols aim to provide unconditional security: the generated key should be secure without making any assumption on the capabilities or knowledge of the attacker. Similarly, when examining the security of a practical implementation, a desired goal is to guarantee the security of the implementation without imposing any conditions or limitations on Eve. In particular, Eve is assumed to be all-powerful and all-knowledgeable, where her knowledge includes the structure of the implementation, and any action Alice and Bob can take as part of the protocol. Under this assumption, we must assume that Eve has knowledge of any vulnerability that exists in the devices used by Alice and Bob, which she can and will exploit in order to conduct her attack.

In contrast, classical cybersecurity considers a wide range of possible adversaries when examining system security. Some (resourceful) adversaries have intimate knowledge of the system’s inner workings, while others do not. Furthermore, even adversaries who know the inner workings of a system may not have detected all its vulnerabilities; the same may be true even for the system designers themselves. Thus, we conclude that many *practical adversaries* and system designers do not know a priori all the vulnerabilities in a specified system.

When an adversary wants to attack a system but does not know of any vulnerability that could be exploited, they can perform *vulnerability research*—a systematic process for identifying existing vulnerabilities. Vulnerability research can be carried out via multiple methods. Some require full knowledge of the internal implementation (such as source code), while others can be applied in a *black-box* manner, independent of the specifics of the implementation.

The same applies when analyzing the security of QKD systems: system designers and attackers might not be fully aware of physical vulnerabilities in a given implementation, making vulnerability research an important tool for identifying vulnerabilities in QKD systems.

In this section, we propose *Quantum Fuzzing*, a simple and effective method for researching vulnerabilities in practical QKD systems.

4.2 Quantum Fuzzing: Definition

The concept of *fuzzing* [42, 25] is a simple yet effective method to conduct vulnerability research on a device, whether classical or quantum, by probing it with various inputs (both valid and invalid) and analyzing the results: how each input affects the device, as well as the device’s output. Adapting this concept to QKD systems, we define Quantum Fuzzing in the following way:

Definition 6. Quantum Fuzzing *is the process of testing a quantum device by sending many quantum and classical states, studying both their effect on the device and the device’s output.*

The concept of Quantum Fuzzing has previously been discussed in the context of quantum software testing [50, 51]. However, here we wish to consider it in a different context: of cybersecurity and vulnerability research for QKD.

4.3 Choosing Input States

All fuzzing algorithms and devices (commonly called “fuzzers”) need an underlying strategy: what test cases should be tried, and which cases should be tried first? Should these choices change based on the device’s output? If so, how?

In classical fuzzing, the subject of fuzzing strategies has been thoroughly researched [52, 53]. Various rules and statistics are used to determine which inputs are likely to yield valuable outcomes and should thus be tested first. In addition, some classical fuzzers use the tested device’s output to improve their test cases mid-run: if a certain input triggers an interesting behavior, it may be beneficial to test other similar inputs, or otherwise to concatenate this interesting input to the next test cases.

Clearly, a fuzzing strategy is also required for Quantum Fuzzing: there are infinitely many states that can be sent to a device, and one must decide which input states to test and in what order. This strategy may be fixed or adaptive, changing the next input based on the device’s responses so far.

An intuitive strategy for fuzzing QKD devices is to begin with valid input states and gradually modify them: starting from simple variations in single degrees of freedom, and progressively moving to more complex modifications. The first test cases should be the valid protocol states, in order to verify that the device responds to them appropriately. Then, the next test cases should add small variations to the valid states. Good candidates for these variations can be inspired by previous, well-known attacks: shifting the frequency of the photons [54], changing their arrival time [23, 27], changing the signal intensity [55, 21], etc. If small variations do not trigger an interesting behavior in the device, the next test cases should perform more complex variations and modify more than one degree of freedom in each test case: for example, changing both the time and frequency of a photon, or testing a broader range of pulse intensities. As test cases progress, one can increase the complexity of modifications to each degree of freedom and combine modifications to more degrees of freedom. If a test case triggers an “interesting” behavior in the device, it should be documented, and potentially combined with other test cases in order to generate more interesting behaviors.

We leave the task of extending this strategy, as well as the task of constructing a physical device that can implement it, for future research.

4.4 Advantages and Limitations of Quantum Fuzzing

The most significant advantage of Quantum Fuzzing is its ability to reveal vulnerabilities without requiring expert knowledge: it can be applied with minimal knowledge of the target device (it only requires the attacker to know the valid input states it is supposed to handle) and can reveal the existence of vulnerabilities that would otherwise require extensive and intimate knowledge of the device to detect. For example, in Section 7 we show how the vulnerability that underlies the Bright Illumination attack [21, 56] could have been found using Quantum Fuzzing.

However, Quantum Fuzzing is not without limitations. The first limitation is its partial coverage: any method that tests a finite number of states cannot guarantee secure behavior under an infinite number of possible input states. Thus, Quantum Fuzzing can help find issues with an implementation, but cannot prove security or guarantee the absence of vulnerabilities.

The second limitation is the imprecise knowledge of the detected vulnerability. Some vulnerabilities occur in internal parts of an implementation. While Quantum Fuzzing can send

an input state that will trigger these vulnerabilities and create some phenomenon that the attacker can witness, the attacker may be unable to deduce which internal part of the device is faulty and what the precise vulnerability is, especially if they lack knowledge of the inner workings of the device.

These two limitations are also true for classical fuzzing. First, since it is impossible to check a program’s behavior under all possible inputs, classical fuzzing also cannot guarantee security. Second, classical fuzzing does not always reveal full details on the detected vulnerability: for example, the mere knowledge that sending a certain message caused a website to crash does not reveal which component of the website caused the crash, the specific vulnerability in the component, or how it could be further exploited.

However, both in classical and quantum systems, even imprecise knowledge of a vulnerability holds great value: it highlights specific aspects and sub-components of the device that should be analyzed more carefully to fully characterize the detected vulnerability.

5 Reversed-Space Attacks

At its essence, the Reversed-Space method characterizes the quantum space that affects the measurements in a QKD scheme. Towards this end, the method analyzes both the measurement done during the QKD scheme as well as their *interpretations* by the parties. By reversing each measured state *backwards* through the implementation, we can obtain the set of states that, if sent to the device, will be measured according to some given interpretation. This forms the attack surface (Definition 1) of the QKD implementation—the possible ways to attack it. By analyzing this attack surface, i.e., the resulting reversed space, we can define possible attacks (exploits, Definition 3) on the implementation and analyze their effectivity.

5.1 Reversed Space Formalism: a Guiding Example

In order to demonstrate the ideas of the Reversed-Space Attack, consider the photonic BB84 implementation of Section 2.2, where Alice sends (via a single pulse) a perfect qubit encoded into the polarization of a single photon. Further suppose that Bob uses a detector that cannot distinguish a single photon from a pair of photons. Then, even though a pair of photons never arrives from Alice in that single pulse (since Alice is assumed to be ideal), the quantum state describing that option could arrive at Bob from an imperfect channel or a channel controlled by Eve, hence, ought to be taken into account.

We now explain the scenario through the lens of the Reversed-Space formalism. Let $\{|j\rangle_B\}_j = \{|1, 0\rangle^F, |0, 1\rangle^F\}$ be the computational basis for Bob’s system. Assume without loss of generality that Bob’s device is described by a unitary transformation U_B , followed by a measurement in Bob’s *computational basis*.³ The unitary transformation U_B , and thus the actual measurement that Bob performs, depends on a random input of Bob, which determines whether Bob measures the computational or Hadamard basis. Namely, to measure in the computational basis, Bob sets $U_B = I$ and measures the result in his computational basis. To measure in the Hadamard basis, Bob lets the pulse go through optical devices such as a polarization rotator, which, on a single qubit, has the effect of performing $U_B = H \triangleq \frac{1}{\sqrt{2}} \begin{pmatrix} 1 & 1 \\ 1 & -1 \end{pmatrix}$; Bob then measures the resulting pulse in the computational basis. Note that U_B is well-defined by the optical device for any arriving state, not only a single-photon “qubit” pulse.

As explained above, Bob actually receives a quantum space of a larger dimension, and his measurement outcomes may be richer than a single bit, as is the case when measuring a qubit. In particular, Bob can interpret his measurement outcome in multiple ways: (i) **information:** when the outcome indicates a specific value sent by Alice. This corresponds, for instance, to

³Any generalized measurement (POVM) can be described as adding an ancilla, measuring, and possibly forgetting (treating several outcomes as the same outcome), and thus is included within our formalization.

the case where Bob receives the state $|1, 0\rangle^F$ or $|2, 0\rangle^F$. (ii) **a loss**: when nothing is measured or when Alice did not send any value. This corresponds to receiving $|0, 0\rangle^F$. (iii) **invalid outcome**: any other situation where the measurement outcome is considered invalid. This corresponds to the case where Bob gets the state $|1, 1\rangle^F$ and both its detectors click.

Once we identify all the relevant states $|j\rangle_B$ measured by Bob, and all possible transformations taken by its device, we can apply the reversed transformation(s) $U_B^{-1} = U_B^\dagger$ on each such state $|j\rangle_B$. These states, $\{U_B^\dagger|j\rangle_B\}$, span the space that influences Bob’s outcome. While Alice and Bob may not be aware of that enlarged space, any security analysis must assume that the attacker is fully aware of it (even if this space is not fully available to an attacker). Indeed, the fact that Bob’s equipment measures and returns a valid result for the state $|2, 0\rangle^F$ may be unknown to Alice and Bob, but known to Eve (e.g., due to analyzing the device or due to fuzzing). When Eve designs her attack, she can consider all the parts of the space spanned by $\{U_B^\dagger|j\rangle_B\}$ that is available to her, and she is not limited to using only ideal qubits as Alice and Bob believe they do.

We call an attack designed according to this observation a *Reversed-Space Attack* for a specific reason: the term “reversed” here is borrowed from the time reversal symmetry of quantum theory. The symmetry of quantum mechanics to the exchange of the prepared (pre-selected) state and the measured (post-selected) state was suggested by [57, 58], and was already used in quantum cryptography as well, see the time-reversed EPR scheme [59] for example. Interestingly, the time-reversed EPR scheme of [59] also leads to more secure protocols, named “measurement-device-independent QKD” [5].

5.2 The Reversed-Space Attack

Throughout the analysis in this section we assume that Alice is ideal. In particular, Alice generates and sends perfect qubits in a two-dimensional space $\mathcal{H}^A = \mathcal{H}_2$, where $\mathcal{H}_2 = \mathbb{C}^2$ is the 2-dimensional Hilbert space corresponding to a single qubit. We denote the basis states of her system by $|i\rangle_A$ with $i \in \{0, 1\}$. Since Alice is ideal, her space is necessarily a subspace of the larger space that affects Bob’s measuring device.

5.2.1 Bob’s Measurement

We formalize Bob’s actions as (i) obtaining a quantum system from the channel; (ii) potentially adding an ancillary quantum system (without loss of generality, in a fixed state $|0\rangle_{\text{anc}} \in \mathcal{H}^{\text{anc}}$, where \mathcal{H}^{anc} is the Hilbert space of the ancillary system). (iii) performing a unitary transformation on the joint system from a fixed set of m possible transformations $\{U_{B_1}, \dots, U_{B_m}\}$; (iv) measuring Bob’s Hilbert space \mathcal{H}^B in a certain basis⁴ B_B .

In order to define the reversed space relevant to this implementation, we start with Bob’s possible outcomes, and we use time reversal to find the exact Hilbert space \mathcal{H}^P which is controlled by Eve and affects Bob’s measurement outcome. First, let \mathcal{H}^B be the span of $\{|j\rangle_B\}$, for all basis states $|j\rangle_B$ measured by Bob. Then, \mathcal{H}^P is defined to be the span of $\{U_{B_s}^\dagger|j\rangle_B\}$, for any $s \in \{1, \dots, m\}$ and all basis states $|j\rangle_B \in \mathcal{H}^B$, after tracing out any ancillary space not available to Eve (resulted from an ancillary space \mathcal{H}^{anc} added by Bob in the “forward in time” description). Any state in Eve’s space that is orthogonal to \mathcal{H}^P goes, after U_{B_s} , to a state which is orthogonal to \mathcal{H}^B and can never affect Bob.

Since in the ideal-Alice case, her Hilbert space \mathcal{H}^A is a subspace of \mathcal{H}^P , we treat Alice’s qubit as the span of two orthonormal states in \mathcal{H}^P .

In the most general case, the resulting reversed space is rather complex, as it can take into account arriving multi-photon states, arriving multi-mode states, and potentially, the ancilla Bob’s device inherently adds. For simplicity, one may analyze each aspect separately, although

⁴When considering qubits, we can assume Bob uses the computational basis, but this may not be the case in some implementations.

for a full security proof, one must take the combined effect into account as well. We next show how Eve's attack translates to our Reversed-Space formalism.

5.2.2 Eve's Attack

Since in practice Bob is affected exactly by \mathcal{H}^P , Eve only needs to attack this extended space. Thus, her most general attack can be described as adding the ancilla $|0\rangle_E$ and performing a transformation U_E on the state $|\psi\rangle_A$ sent by Alice. Note that Alice state is actually embedded in \mathcal{H}^P , hence, Eve acts on $|\psi\rangle_A \rightarrow |\psi\rangle_P = \sum_i \alpha_i |i\rangle_P \in \mathcal{H}^P$ (where the arrow stands for an embedding). Eve's actions can thus be written as,

$$|0\rangle_E |\psi\rangle_P = \sum_i \alpha_i |0\rangle_E |i\rangle_P \xrightarrow{U_E} \sum_{i,k} \alpha_i \epsilon_{i,k} |E_{i,k}\rangle_E |k\rangle_P. \quad (2)$$

Thus, although Alice's (BB84) state is completely represented by the four simple options $\{\alpha_0 = 1; \alpha_1 = 0\}, \{\alpha_0 = 0; \alpha_1 = 1\}, \{\alpha_0 = 1/\sqrt{2}; \alpha_1 = 1/\sqrt{2}\}, \{\alpha_0 = 1/\sqrt{2}; \alpha_1 = -1/\sqrt{2}\}$, the state right after Eve's attack is much more complex.

Eve then sends a state in \mathcal{H}^P to Bob, who processes it as explained above. We can formulate Bob's action on any basis state $|k\rangle_P$, for a given setting U_{B_s} with $s \in \{1, \dots, m\}$, by

$$|k\rangle_P |0\rangle_{\text{anc}} \xrightarrow{U_{B_s}} \sum_j \beta_{k,j}^s |j\rangle_{P \otimes \text{anc}}, \quad (3)$$

leading to the final state $|\Psi_{EB}\rangle$ that Bob and Eve hold at the end of the process (just before Bob measures)

$$|\Psi_{EB}\rangle \triangleq \sum_{i,k,j} \alpha_i \epsilon_{i,k} \beta_{k,j}^s |E_{i,k}\rangle_E |j\rangle_{P \otimes \text{anc}}, \quad (4)$$

derived through Eqs. (2)–(3),

$$\begin{aligned} |\psi\rangle_P &\longrightarrow |0\rangle_E |\psi\rangle_P \xrightarrow{U_E} \sum_{i,k} \alpha_i \epsilon_{i,k} |E_{i,k}\rangle_E |k\rangle_P \\ &\longrightarrow \sum_{i,k} \alpha_i \epsilon_{i,k} |E_{i,k}\rangle_E |k\rangle_P |0\rangle_{\text{anc}} \xrightarrow{U_{B_s}} \sum_{i,k} \alpha_i \epsilon_{i,k} |E_{i,k}\rangle_E \sum_j \beta_{k,j}^s |j\rangle_{P \otimes \text{anc}}. \end{aligned}$$

Finally, Bob measures the space \mathcal{H}^B using his basis. Note that $\mathcal{H}^B \subseteq \mathcal{H}^P \otimes \mathcal{H}^{\text{anc}}$.

5.2.3 Bob's Interpretation and Oblivious Attacks

In QKD implementations, the way Bob interprets his measurement outcome is of great importance. The states $|j\rangle_B$ can be classified into sets according to Bob's interpretation: some of these states indicate "Alice has sent the bit 0", while others indicate "Alice has sent the bit 1". Let us denote the set of (basis) states that Bob interprets as measuring the bit value 0 by J_0 and the set of states interpreted as a 1 by J_1 .

When Alice sends a bit b , but Bob measures a state in J_{1-b} , the transmission is said to be an *error*. Generally, for a specific transmission, we define J_{error} as the set of all states that Bob regards as an error. Note that these sets are defined *per transmission* and depend on the specific basis Bob uses and the state Alice sends (i.e., the bit value b she communicates).

When considering real implementations, there may be some outcomes that are not interpreted as valid outcomes since they never happen in the "ideal" scheme. These outcomes can be divided into two groups, according to Bob's interpretation:

1. *Outcomes interpreted as a loss*: transmissions that can naturally occur but supply no information to Bob. For example, vacuum pulses that make no detector click, or measurement results that are inconclusive and are part of the theoretical protocol (as occurs in the B92 protocol [2]). These outcomes are denoted as the set J_{loss} .
2. *Invalid-erroneous outcomes*: outcomes that can never occur if the quantum system sent by Alice reaches Bob intact (e.g. when several detectors click, while Alice is guaranteed to send a single photon). These outcomes are denoted as the set J_{invalid} .

The collection of all $J_0, J_1, J_{\text{loss}}$ and J_{invalid} sets for a certain receiver implementation are called *the interpretation sets* of the receiver.

It is Bob's choice of interpretation that determines whether a specific outcome is considered a loss or an invalid result. Generally speaking, when an invalid outcome increases Bob's measured error rate, we put it in the set J_{invalid} , and when it is ignored by Bob, we put it in J_{loss} . As an example, let us consider the case where Alice's state generation is not totally ideal, and she can either send a single photon or, at most, two photons. If Bob treats these cases of noticing many photons as a loss (i.e., he ignores that transmission, thus this measurement is in J_{loss}) rather than as an error, this results in a major security hole [55, 60].

We call attacks that cause no errors and no invalid outcomes at Bob's end "oblivious". That is, we require that for any $|j\rangle$ in J_{error} or in J_{invalid} , the overlap $\langle j|\Psi_{\text{EB}}\rangle$ is zero, so Bob never measures $|j\rangle$. We formalize this idea using the description of the final state shown in Eq. (4) in the following manner:

Observation 1. *For a given QKD implementation, Eve's attack U_{E} causes no errors if and only if for every state $|\psi\rangle = \sum_i \alpha_i |i\rangle_{\text{P}}$ sent by Alice and for any U_{B_s} used by Bob, it holds that*

$$\sum_{i,k} \alpha_i \epsilon_{i,k} \beta_{k,j}^s |E_{i,k}\rangle_{\text{E}} = 0, \quad (5)$$

for any $j \in J_{\text{error}} \cup J_{\text{invalid}}$ (determined according to the specific $|\psi\rangle$ sent by Alice, and the specific setting s used by Bob).

To clarify the notations for oblivious attacks, let us provide a simple example and show that a CNOT attack made by Eve does not satisfy the conditions of Observation 1 and thus can be noticed by Bob. For instance, consider a standard BB84 scheme [1] in which Bob's setup for the computational basis is $U_{\text{B}_C} = I$ the identity, and for the Hadamard basis, $U_{\text{B}_H} = H$ is Hadamard transformation; both are followed by a measurement in the computational basis. Assume Alice sends $|\psi\rangle_{\text{A}} = |+\rangle$, but Eve performs a CNOT attack using the computational basis. After the attack, the system (Alice's qubit and Eve's added ancilla) is in the state $|\tilde{\psi}\rangle = (|E_{0,0}\rangle_{\text{E}}|0\rangle_{\text{P}} + |E_{1,1}\rangle_{\text{E}}|1\rangle_{\text{P}})/\sqrt{2}$ with orthogonal $|E_{0,0}\rangle_{\text{E}}$ and $|E_{1,1}\rangle_{\text{E}}$. Assume Bob sets his apparatus to the Hadamard basis (same as Alice). Thus, he applies the Hadamard transformation, and measures subsystem P of the resulting state $|\Psi_{\text{EB}}\rangle = (I_{\text{E}} \otimes U_{\text{B}_H})|\tilde{\psi}\rangle = (|E_{0,0}\rangle_{\text{E}}|+\rangle_{\text{P}} + |E_{1,1}\rangle_{\text{E}}|-\rangle_{\text{P}})/\sqrt{2}$ in the computation basis. We now show that Bob has a positive probability of measuring $|1\rangle$ (that is, $j = 1$), while this outcome is in J_{error} and indicates an error: using the formulation of Observation 1, Alice's qubit is given by $\alpha_0 = \alpha_1 = 1/\sqrt{2}$, Eve's attack by $\epsilon_{0,0} = \epsilon_{1,1} = 1$ and $\epsilon_{0,1} = \epsilon_{1,0} = 0$ and Bob's setup by $\beta_{0,0}^H = \beta_{0,1}^H = \beta_{1,0}^H = 1/\sqrt{2}$ and $\beta_{1,1}^H = -1/\sqrt{2}$. Indeed, Eq. (5) for $j = 1$ gives $\sum_{i,k \in \{0,1\}} \alpha_i \epsilon_{i,k} \beta_{k,1}^H |E_{i,k}\rangle_{\text{E}} = \frac{1}{\sqrt{2}} \cdot 1 \cdot \frac{1}{\sqrt{2}} |E_{0,0}\rangle + \frac{1}{\sqrt{2}} \cdot 1 \cdot \frac{-1}{\sqrt{2}} |E_{1,1}\rangle$, which is non-zero since $|E_{0,0}\rangle$ and $|E_{1,1}\rangle$ are orthogonal.

Finally, we can define the set of *oblivious* attacks that are "unnoticeable" by the parties.

Definition 7. *Let \mathbf{U}_{zero} be the set of attacks on a given protocol, that cause no errors (in all the possible setups of the protocol).*

Any attack in \mathbf{U}_{zero} that leaks some information to Eve is considered a successful attack that potentially damages the security of the implemented QKD scheme.

5.3 Example: a Complete Reversed-Space Attack

A detailed example of a Reversed-Space Attack on a time-based interferometric BB84 scheme, which yields an oblivious attack on that implementation, is given in Appendix B. This subsection gives a short overview of the attack.

In the attacked implementation, Alice encodes her qubit using time-bin encoding with two time-bins (denoted t'_0 and t'_1). However, Bob's implementation measures *six* different modes in order to perform his measurement: three different times in the two arms of an interferometer. Furthermore, Reversed-Space analysis reveals that Bob's measurement can be affected by two additional times, denoted t'_{-1} and t'_2 .

When analyzing Bob's interpretation of the two additional times, it is revealed that pulses in the two additional times *force* Bob to measure in the basis of Eve's choice (or experience a loss of the signal).

Finally, Eve uses these additional states and their interpretation to construct an attack that has zero chance of generating an erroneous measurement in Bob's system.

This attack breaks the security (and the robustness: see [61]) of the implementation, because Eve gains *full* information on the key without inducing any error and without causing the protocol to abort.

Another successful reversed-space attack on a polarization-based interferometric BB84 implementation has been reported in [24].

5.4 Discussion: Countermeasures to Reversed-Space Attacks

Can Bob measure more states to defend against attacks on the enlarged space coming from Eve? Although this seems like a natural countermeasure, it may in fact add vulnerabilities that were not originally present and open a path for new attacks: now Bob's measured space is larger, and so is its reversed space! Hence, when analyzing the security of an implementation, one must *fix* Bob's implementation before letting Eve attack it. If we modify Bob to counter an attack, the analysis must be repeated on the new implementation, considering the new dimensions measured by Bob and his new interpretation of outcomes.

In Appendix C we revisit the Reversed-Space Attack on interferometric BB84 that was described in Appendix B, while adding the countermeasure of measuring additional time bins in Bob's implementation. On the one hand, our analysis shows that, under the restriction of Eve to sending single-photon pulses and non-collective attacks, Bob's given device is effective in blocking Reversed-Space Attacks. On the other hand, we demonstrate that the additional modes measured by Bob effectively create a new implementation with a different, larger reversed space. Eve can now use a broader range of attacks than before on this new implementation.

5.5 Other Examples of Reversed-Space Attacks

In Appendix D.1 we analyze the setting described in Example 1 of Section 3.2.1 using the Reversed-Space method. This setting is known to be exposed to attacks that are, in fact, a special case of Reversed-Space Attacks.

In Appendix D.2 we revisit the setting of Section 5.3 where Bob measures six modes in the interferometric setup. Now, we restrict Bob to measuring only two modes: the middle time-bin of each interferometer arm. We design an attack that is much stronger than the attack presented in Section 5.3. Its existence strengthens the conclusions presented in Section 5.4, which imply that modifying the measurement scheme of a QKD implementation needs to be thoroughly analyzed.

5.6 Summary: Reversed-Space is an Exploit

We conclude by making the following observations, which connect the reversed-space attack to our cybersecurity analysis framework depicted in Section 3.

Observation 2. *Knowing the Measurement Space Vulnerabilities of Bob’s device allows the computation of the reversed space, which is a part of Bob’s attack surface.*

By definition, Measurement Space Vulnerabilities (Definition 4) reveal the large, realistic Hilbert space that Bob measures. The reversal of said space through Bob’s setup is exactly the Hilbert space of states that Eve can send to affect Bob. As discussed in Section 3.2.2, this is the state space part of Bob’s attack surface.

Observation 3. *The computation of the “zero noise requirement” in a Reversed-Space Attack is based on Interpretation Vulnerabilities.*

Interpretation Vulnerabilities, by Definition 5, reveal additional information on how Bob interprets his incoming states; specifically, they reveal interpretations that should not exist in an ideal protocol, and are necessary information for Eq. (5) that defines the “zero noise requirement”. These interpretations are often the key to the success of the attack.

The following observation follows directly:

Observation 4. *Reversed-Space is a generic exploit for Measurement Space Vulnerabilities and Interpretation Vulnerabilities.*

Reversed-Space Attacks, as an exploit method, are usable both for an attacker seeking to exploit a vulnerability (either publicly known or known only to him), and for system designers checking the practical security of their QKD implementation.

6 Quantum Side-Channel Attacks

In this section, we examine side-channel attacks, which exploit unintended physical interfaces to compromise security, in the context of QKD devices. As classical intuition fails to capture the nature of side channels in QKD devices, we introduce a new definition of “Quantum Side-Channel Attacks”. Through concrete examples, we show that Quantum Side-Channel Attacks can target a wide range of device components. Because these attacks are often overlooked in standard security analyses, our definition emphasizes the need to treat them explicitly, providing system designers with a clearer understanding and a stronger basis for defending against them.

6.1 The Classical Concept of Side-Channel Attacks

In cybersecurity, side-channel attacks are attacks on computing systems that utilize unconventional interfaces exposed by the target system. An attack can use these interfaces to extract data from the system, as well as modify the system’s behavior.

The most common examples of these interfaces are the physical aspects of the system implementation, such as execution time, electromagnetic radiation, and power consumption. For example, by measuring the exact duration of a cryptographic computation, an attacker can deduce information about the secret key used in the computation [62, 63]. In another example, electromagnetic radiation was applied to a tamper-resistant device to trigger faults in its computation, modifying its behavior and revealing information on the device’s secret key [64, 65].

In fact, side-channel attacks that use physical imperfections are so common that some consider an attack to be a side-channel attack *if and only if* it is based on the physical implementation of the device [66].

6.2 Adapting Side-Channel Attacks to QKD

As part of our analysis of QKD systems through cybersecurity concepts and methodologies, we can apply the notion of side-channel attacks to QKD systems.

Previous works have used intuition from classical cybersecurity and referred to all attacks on QKD systems that utilize physical imperfections as “side-channel attacks” (see, e.g., [55, 67]). However, there is a clear issue with this approach: it classifies almost every attack as a “side-channel attack”, rendering the definition useless. In QKD implementations, the device that prepares the signals and the device that measures them perform a physical process, and the signals themselves are physical, photonic pulses. Thus, if the criterion for a side-channel attack is to utilize physical imperfections, any attack that utilizes an imperfection in the preparation device, the measurement device, or the signals is a side-channel attack.

We resolve this issue by changing the focus on what defines an interface as a side channel: instead of focusing on the physics of the implementation, we focus on what interfaces should (and should not) be exposed in a device. Once we understand what interfaces a QKD device intends to expose, we can understand what the unconventional interfaces of the device are, and, respectively, what should be considered a side channel.

In a transmitting device (Alice), the conventional interface is the device’s transmissions: the space of states that the device can transmit. In a measuring device (Bob), the conventional interface is the device’s measurement of incoming signals, which is modeled as the space of states that Bob measures (or that affect Bob’s measurement). Thus, we view side-channel attacks on QKD as attacks that depend on more than Alice’s sent states, or affect something other than Bob’s measured space (or the ancillas Eve can save inside her system). We arrive at the following definition:

Definition 8. *An attack is a Quantum Side-Channel Attack if:*

1. *either its input depends non-trivially on more than Alice’s sent states,*
2. *or its output non-trivially affects more than Bob’s measured space and the attacker’s private ancillas.*

A full, formal definition, based on the Hilbert spaces that each device uses, can be found in Appendix E.

There have been past attempts to classify attacks on QKD implementations that do not rely on the conventional interfaces of the devices. Vakhitov, Makarov, and Hjelme [17] used the term “conventional optical eavesdropping” to describe attacks where “... *Eve can get information by using loopholes in Alice’s and Bob’s optical set-up rather than by measuring the transmitted quantum states.*” This term is, in fact, a special case of our definition. While forcing leakage from the optical setups of Alice and Bob certainly qualifies as a side channel, our definition does not require that we not measure the transmitted quantum states. In fact, as shown below, several Quantum Side-Channel Attacks collect data from QKD devices through side channels, or manipulate QKD devices through side channels, in order to perform more successful measurements of the transmitted quantum states. Furthermore, there are other elements besides the optical setup that can be used to launch a Quantum Side-Channel Attack, as explored below.

6.3 Examples

We will now analyze several examples of attacks on QKD implementations under our new definition.

6.3.1 Quantum Side-Channel Attacks

The Large Pulse attack [17]: This attack works against QKD devices where the legitimate party’s private choices (specific state for Alice, measurement basis for Bob) affect the device’s

optical configuration. In this attack, Eve sends a high-intensity pulse to the device and uses the reflected light to determine the private choice. If Eve learns the used basis (from either Alice or Bob), she can use this data to perform a perfect measure-resend attack. If she learns Alice's chosen state, no further action is required. Since this attack depends on more than Alice's sent states (specifically, the device's optical configuration), it is a Quantum Side-Channel Attack.

The Injection-Locking attack [22]: In this attack, Eve uses specialized pulses that enter Alice's laser, forcing each of Alice's pulses to have a different wavelength depending on the encoded qubit state. This allows Eve to measure the frequency of each transmission and learn Alice's bit perfectly. Since this attack affects Alice's device operation, it is a Quantum Side-Channel Attack.

The Bright Illumination attack [21]: We analyze the Bright Illumination attack in Section 7 and show it to be a Quantum Side-Channel Attack.

6.3.2 Non-Side-Channel Attacks

The photon-number splitting attack [16]: This attack, discussed in Section 3.2.1, utilizes a vulnerability in Alice's transmitter, which makes Alice's sent states sometimes include more than one photon. Eve checks the number of photons in a pulse, and if there is more than one, she saves it as her private ancilla and sends the rest to Bob. Eve measures her saved photon after the bases are published, gaining perfect knowledge of the secret bit. Since the attack only utilizes Alice's signal and generates states that Bob can measure, it is *not* a Quantum Side-Channel Attack.

The Time-Shift attack [23]: This attack works against receivers with different detectors for different bit values, where the detection sensitivities of each detector are unequal. Eve selectively delays Alice's signal, independently of Alice's choice of state, to make one bit value much more likely in Bob's detection. The input of the attack is exactly Alice's signal, and the output of the attack is time-shifted states, inside the space of states that Bob's device can measure. As such, the Time-Shift attack is *not* a Quantum Side-Channel Attack.

Reversed-Space Attack example from Section 5.3: This attack was deliberately constructed to affect all of (and only) the extended Hilbert space that affects Bob's measurement, and it does not depend on any input other than Alice's signal. As such, this attack too is *not* a Quantum Side-Channel Attack.

Further classification of attacks under the Quantum Side-Channel Attack definition can be found in Section 8.

6.4 Application to Security Analyses

As shown in the subsection above, a wide variety of side channels can be used to attack QKD implementations. For an implementation to be proven secure, all these side channels must be considered in the theoretical model of the implementation, though we are not aware of security proofs that use this full modeling. Alternatively, a separate engineering analysis can examine the physical QKD device and its potential side channels and ensure that these side channels cannot be exploited by Eve.

7 Putting It All Together: Analysis of the Bright Illumination Attack

In this section, we analyze the “Bright Illumination” attack and its inner workings using the novel tools we presented in the previous sections. We show that a structured security analysis could have found the Bright Illumination attack, using the tools we propose in this paper and based on an understanding of the importance of practical vulnerability research.

7.1 The Bright Illumination Attack

The “Bright Illumination” attack [31, 21, 68, 56] is an implementation attack that changes the behavior of QKD receivers by exposing them to high-intensity light. This attack was implemented against a variety of QKD implementations, including implementations from recent years [69, 70], using various photodetectors and implementing various protocols [71, 72]. In this section we analyze the specific attack and implementation shown in [56]; however, our analysis can be applied with minor modifications to other Bright Illumination attacks against various QKD implementations.

Receiver Structure In the QKD system targeted by [56], the implemented protocol is polarization-based BB84, and measurement is performed using a passive basis choice and four detectors, as shown in Figure 1a.

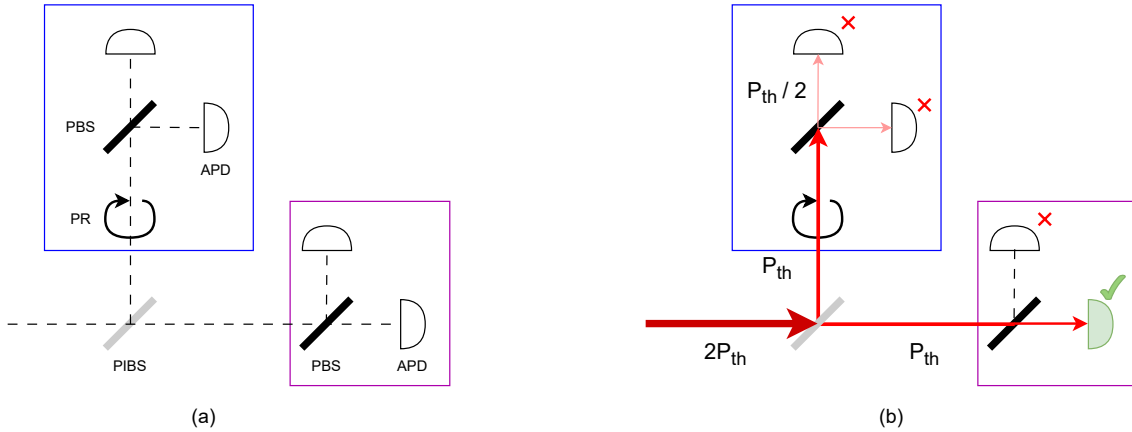


Figure 1: (a) Structure of the QKD receiver targeted in the Bright Illumination attack. PIBS: polarization-independent beam splitter. PBS: polarizing beam splitter. PR: polarization rotator. APD: avalanche photodiode. (b) Propagation of Eve’s high-intensity pulse through the QKD receiver.

The passive basis choice in the receiver is implemented using a polarization-independent beam splitter, which leads to two sub-components. Each sub-component measures in a different basis: the computational basis measurement (marked in purple) is performed using a polarizing beam splitter and two detectors, one in each output arm. The Hadamard basis measurement (marked in blue) is performed in the same way, with the addition of a polarization rotator before the beam splitter to transform the Hadamard basis states into computational basis states.

The detectors used in this implementation are Avalanche Photodiodes (APDs).

APDs have two possible modes of operation, called the “Geiger mode” and “linear mode” [31]. In Geiger mode, an APD operates as a single-photon detector: it generates a “click” (a macroscopic event) when it receives one or more photons. However, in linear mode, the APD “clicks” only if the incoming pulse’s intensity is above a certain threshold: if the pulse intensity is

below that threshold, no effect is registered in the APD (there is no click). Thus, an APD in linear mode is “blind” to low-intensity pulses, including single photons.

In QKD setups, APDs operate in Geiger mode as single-photon detectors. However, an APD can be forcibly reconfigured to linear mode if it is bombarded with high-intensity light (or, potentially, by heating the APD [68]).

Attack Structure The Bright Illumination attack (shown in [56]) relies on APDs having an undesired, linear mode of operation, and the ability to force an APD to operate in the linear mode by sending high-intensity light to it.

In the attack, Eve sends high-intensity light pulses to Bob’s device *before* the intended detection window. This makes the APDs operate in linear mode during the detection window, making them blind to low-intensity pulses. Once the APDs are in linear mode, Eve performs the “measure-resend” attack described in Figure 1b: she picks a specific measurement basis, measures Alice’s signal in that basis, and then generates a signal in the same polarization whose intensity is slightly above $2P_{th}$, where P_{th} is defined as the minimal intensity the APDs can detect in linear mode.

When the pulse enters the polarization-independent beam splitter in Bob’s device, it is split into two pulses with intensity slightly higher than P_{th} . In the sub-component that measures in the basis Eve chose, the polarizing beam splitter will transfer the entire pulse to one arm, which will cause a click in the intended detector. In the other sub-component, the polarizing beam splitter will split the pulse into two parts with intensity around $P_{th}/2$, which will not cause a click in either detector.

Thus, Eve’s attack results in a guaranteed click in a detector of her choosing, causing Eve and Bob to receive the same measurement results. Using this information, Eve can mimic Bob’s classical process by listening to the classical channel. This leaves Eve with full knowledge of the final key when the protocol concludes.

7.2 Is Bright Illumination a Quantum Side-Channel Attack?

As discussed in Sections 7.1 and 7.3, the Bright Illumination attack depends on two separate stages: the first stage is to modify the behavior of Bob’s device (causing the APDs to switch to the linear mode), and the second stage is a measure-resend attack on the modified device. Since in the first stage of the attack, Eve sends blinding pulses that change the behavior of the device (and are not simply measured), the Bright Illumination Attack is a Quantum Side-Channel Attack according to Definition 8.

7.3 Finding the Vulnerabilities via Quantum Fuzzing

In this subsection, we show that applying Quantum Fuzzing to the QKD implementation shown above can reveal the vulnerabilities enabling the Bright Illumination attack.

When using the Quantum Fuzzing strategy defined in Section 4.3, the procedure begins by testing valid protocol states and then gradually modifies certain elements in the states. We start by performing a small set of modifications, and if the results do not expose interesting behavior, we continue by testing either a broader range of values or additional values inside the existing range. Since our fuzzing strategy modifies the intensity of pulses relatively early in the procedure, the following property will be revealed after a few test cases:

Property 1. *Blinding.* *Sending a high-intensity pulse to Bob’s device causes a loss, instead of burning the device or showing an invalid result (such as a click in two detectors at the same time).*

As described in Section 7.1, this effect is caused by the bright pulse forcing Bob’s APDs into the linear mode. This result is highly unexpected: as the intensity of the incoming pulse

increases, one should expect the chance of pulse detection to be higher — but our high-intensity pulse does not cause a detection event at all.

If the Quantum Fuzzing process were to stop after this observation, the useful nature of the linear mode would not be revealed. However, as defined in Section 4.3, if a test case triggers an “interesting” effect on a device, our strategy suggests combining it with other test cases, in the hope of expanding the effect. Employing this strategy, we would send input states that include a high-intensity pulse, followed by another photon pulse. When we test various intensity values for the second pulse, gradually increasing the intensity range and granularity, we reveal two more properties, one after the other:

Property 2. *Weak Pulses under Blinding.* *Sending a high-intensity pulse to Bob’s device, followed by another pulse with a small photon number, will not cause a detection event.*

Property 3. *Strong Pulses under Blinding.* *Sending a high-intensity pulse to Bob’s device, followed by another pulse with a high photon number, will always cause a detection event in the detector matching the pulse’s polarization, and not in detectors used for the other basis.*

These two properties reveal how Bob’s device acts when it is “blinded” (that is, when the APDs in Bob’s device are in the linear mode). In fact, these properties reveal Measurement Space Vulnerabilities and Interpretation Vulnerabilities in Bob’s device (as defined in Section 3.2.1): when Bob’s device is blinded, it measures four states (the high-photon-number variants of the BB84 states) that it should not measure, and interprets them as valid if they match his basis choice, or as a loss if they do not match his basis choice.

Now that we have revealed the Measurement Space Vulnerabilities and Interpretation Vulnerabilities in the device, we can build an exploit for them using the Reversed-Space method.

7.4 Applying Reversed-Space

In the previous subsection, we used Quantum Fuzzing to find a set of Measurement Space Vulnerabilities and Interpretation Vulnerabilities. We now wish to build a Reversed-Space Attack using these vulnerabilities, according to the procedure described in Section 5. For the sake of readability, the computation can be found in Appendix F. The result of the computation is an attack of the form:

$$\begin{aligned} U_E|0\rangle_E|0\rangle_A &= p|E_0\rangle|0\rangle^{\text{bright}} + q|E_2\rangle|+\rangle^{\text{bright}} + q|E_3\rangle|-\rangle^{\text{bright}}, \\ U_E|0\rangle_E|1\rangle_A &= p|E_1\rangle|1\rangle^{\text{bright}} + q|E_2\rangle|+\rangle^{\text{bright}} - q|E_3\rangle|-\rangle^{\text{bright}}, \end{aligned} \quad (6)$$

where p and q are non-negative real numbers that satisfy

$$p^2 + 2q^2 = 1 \quad (7)$$

and the state $|\psi\rangle^{\text{bright}}$ is a high-photon-number variant of the single-photon state $|\psi\rangle$.

To give some intuition to the result, choosing $p = 1$, $q = 0$ gives a CNOT attack from Alice’s computational states to the “blinding-computational” states. Choosing $p = 0$, $q = \frac{1}{\sqrt{2}}$ gives a CNOT attack from Alice’s Hadamard states to the “blinding-Hadamard” states. Intermediate attacks with $0 < p < 1$, $0 < q < \frac{1}{\sqrt{2}}$ resemble the original Bright Illumination attack, which sometimes sends high-photon-number computational basis states and sometimes sends high-photon-number Hadamard basis states.

Similarly to Section 5.3, this attack breaks the security (and the robustness: see [61]) of the implementation, because Eve gains *full* information on the key without inducing any error and without causing the protocol to abort.

The computation of this attack completes the proof that Bright Illumination attacks can be constructed as Reversed-Space Attacks, using vulnerabilities found via Quantum Fuzzing: a system designer with black-box access to the QKD system and no knowledge of its internal workings could have constructed the full attack.

8 Applicability to Current Implementation Attacks

In this section, we explore the relationship between different QKD attacks and the novel methodologies and concepts defined in this paper. Our goal is to provide a broader context for our results and emphasize their usefulness in classifying existing attacks.

To illustrate the relationships between different attacks on QKD implementations and our methodologies, we present a visual diagram in Figure 2, accompanied by an explanation of the results and insights presented in the diagram. High-level details on each attack in the diagram can be found in Appendix G.

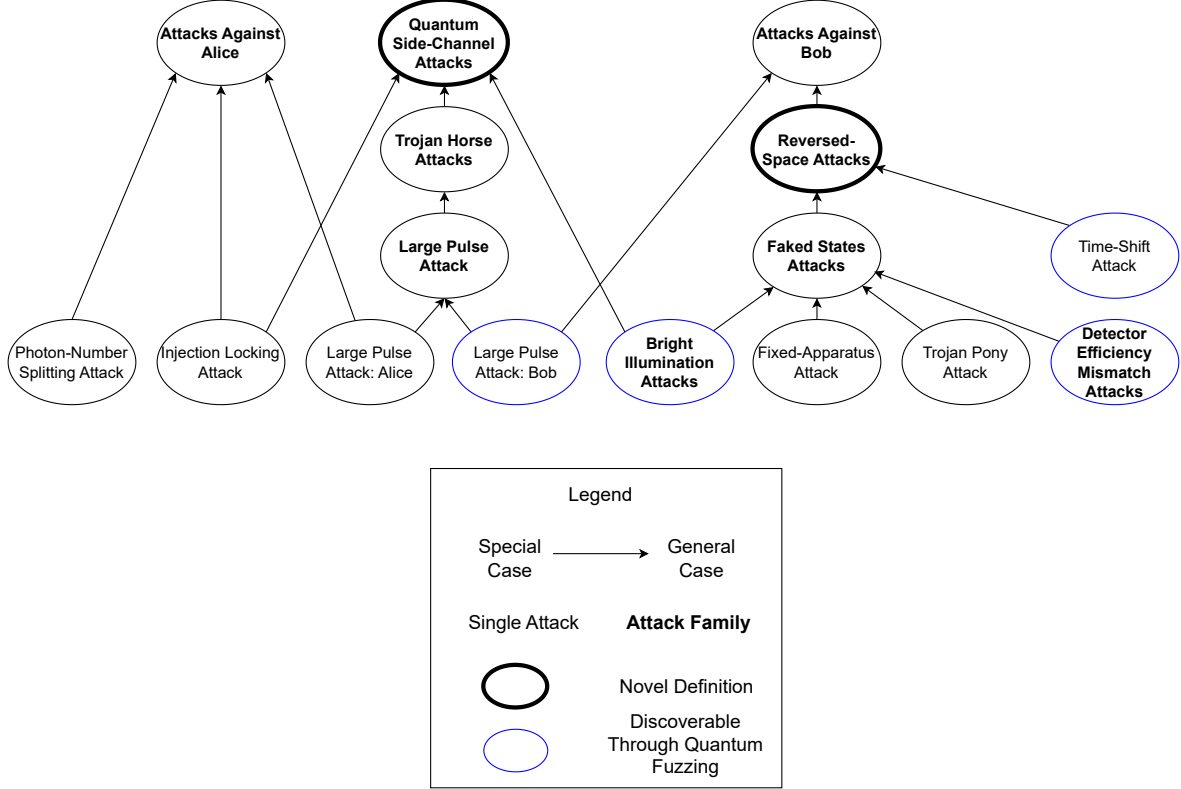


Figure 2: A representation of the relations between QKD attacks and our results.

The diagram is constructed as a graph, where each node represents an attack (or attack family), and an edge from one node to another means that the former is a special case of the latter.

We will now discuss the relations between existing QKD attacks and each of our results separately.

8.1 Relationship to Quantum Side-Channel Attacks

Observation 5. *There are Quantum Side-Channel Attacks against Alice and against Bob, but non-side-channel attacks also exist for both.*

The diagram, as well as Section 6.3, show that Quantum Side-Channel Attacks are not only a theoretical definition: there are several practical examples of Quantum Side-Channel Attacks, both against Alice and against Bob, such as the Large Pulse attacks, the Injection Locking attack, and the Bright Illumination attacks.

However, in contrast to earlier definitions of side-channel attacks in QKD (see, e.g., [55]), our definition does not capture all implementation attacks: many (if not most) well-known examples do not use elements that are external to Alice and Bob’s protocol, and thus do not fall

under our definition. Examples of such attacks are the Photon-Number-Splitting attack, the Trojan Pony attack, and the Time-Shift attack. Hence, our definition of Quantum Side-Channel Attacks represents a class of special, yet practical implementation attacks.

8.2 Relationship to Reversed-Space Attacks

Observation 6. *Reversed-Space Attacks are a strict generalization of Faked-States attacks, and include some Quantum Side-Channel Attacks, but do not include all attacks against Bob.*

Reversed-Space Attacks are a generalization of Faked-States attacks for the following reason: since Faked-States attacks rely on the existence of “faked states” that force a specific interpretation in Bob’s measurement device, they rely on Measurement Space Vulnerabilities and Interpretation Vulnerabilities. Hence, all Faked-States attacks are in particular Reversed-Space Attacks. However, the opposite is not true: the Time-Shift attack is a Reversed-Space Attack which is not a Faked-States attack, because it depends on an enlarged measured space, but it does not measure Alice’s signal as is required in Faked-States attacks [19].

The Bright Illumination attack shown in Section 7 is an example of a Reversed-Space Attack that is also a Quantum Side-Channel Attack.

Finally, the Large Pulse attack (against Bob) is an example of a non-Reversed-Space Attack against Bob, since it does not depend on an enlarged measurement space in Bob’s interpretation.

8.3 Relationship to Quantum Fuzzing

Observation 7. *Quantum Fuzzing can discover both Quantum Side-Channel Attacks and non-side-channel attacks, but cannot discover all attacks against Bob. Furthermore, our current strategy cannot be applied against Alice’s device.*

Since Quantum Fuzzing tests the behavior of a device by sending different input states to it, it can reveal the vulnerabilities behind several attacks. Four attacks that are triggered by sending specific input states to Bob’s device are the Large Pulse attack (against Bob), the Bright Illumination attacks, the Detector Efficiency Mismatch attacks, and the Time-Shift attack. The first two attacks are examples of Quantum Side-Channel Attacks, and the last two attacks are not Quantum Side-Channel Attacks.

However, not all attacks against Bob can be found via Quantum Fuzzing, since some attacks rely on elements that are outside of the device’s input channel. For example, the Fixed-Apparatus attack that uses the blocked arm inside Bob’s device, which is not available through the input channel.

Additionally, since our Quantum Fuzzing strategy relies on the existence of valid protocol states as initial test cases, and Alice’s device is not supposed to receive any outside input, our strategy cannot be applied to discover attacks against Alice. However, a different Quantum Fuzzing strategy can potentially reveal attacks on Alice’s device that require external input from Eve, such as the Injection Locking attack and the Large Pulse attack (against Alice).

9 Conclusions and Future Work

Our work defines a quantum cybersecurity approach for systematically analyzing the security of QKD implementations, inspired by cybersecurity research on classical computing systems. We have shown a fundamental connection between imperfections and attacks on QKD implementations, and the classical notions of vulnerabilities, attack surfaces, and exploits (Section 3). We have also defined common vulnerability types in QKD devices, shown the role of attack surfaces in the feasibility of attacks on QKD devices, and examined generic exploit methods for implementation attacks.

Expanding on the connection between classical cybersecurity and QKD implementations, we have presented three additional contributions. First, through our definition of Quantum Fuzzing (Section 4), which is the first vulnerability research method for QKD implementations, QKD system designers can search for issues in their implementation that they did not know existed. Second, our Reversed-Space Attacks methodology (Section 5) is a new generic exploit which computes and utilizes the QKD receiver’s attack surface, allowing system designers and attackers to build more sophisticated implementation attacks. Third, our definition of “Quantum Side-Channel Attacks” (Section 6) accounts for the special nature of side channels in QKD devices, and emphasizes that the security of QKD devices can be compromised by elements outside of Alice’s transmission and Bob’s measurement.

The paper concludes with two additional applications of our newly-defined concepts and methodologies. First, we have revisited the Bright Illumination attack (Section 7) and demonstrated how our tools could have predicted this attack through a rigorous security analysis. Second, we have classified existing attacks using our new definitions (Section 8), emphasizing the applicability of our tools to a large number of attacks and attack families.

The goal of our work is to create a connection between classical and quantum implementation attacks and allow greater collaborations between classical cybersecurity experts and QKD experts. Quantum researchers can borrow approaches and results from classical cybersecurity in order to define new attacks and defend against them. Cybersecurity researchers can understand attacks on QKD implementations through their own perspective and apply their personal experience and expertise. This, in turn, can greatly improve the practical security of experimental and commercial QKD devices.

By building new tools for analyzing threats from practical adversaries, we aim to bridge the gap between practical QKD security research that only deals with all-knowing, all-powerful adversaries and classical cybersecurity that often deals with realistic, limited adversaries and what they can achieve. The benefits of this added perspective are clear: for instance, awareness of the need to do vulnerability research, together with the tools for exploiting space-enlargement vulnerabilities, could have revealed the Bright Illumination attack and enabled QKD system designers to discover it before potential adversaries. More importantly, these tools can help discover further attacks in the future.

Since our work focuses on attacks on imperfect QKD devices, one may try to partially solve the problem by using QKD protocols with an untrusted center party (typically named Charlie): since an untrusted party is assumed to be malicious, imperfections in its implementation cannot harm security. However, even in such protocols, imperfections in the trusted parties can still harm security, and our tools can still be used to analyze them. While entanglement-based protocols (such as BBM92 [73]) protect against state generation imperfections, attacks against the measurement device (such as Reversed-Space Attacks) are still possible. Similarly, in protocols with measurement by an untrusted center (such as BHM96 [59] or MDI-QKD [5]), attacks against the state preparation devices (such as the Photon-Number-Splitting and Large Pulse attacks [16, 17]) are still possible. While Device-Independent QKD protocols [74] assume *all* devices to be untrusted and thus theoretically secure against implementation attacks, they still depend on many assumptions, including the assumption that Alice and Bob’s input choices are random and independent. Failure to satisfy these assumptions in practical implementations can, in fact, compromise the security of the protocol, as seen, for example, in [75].

Several directions we consider promising for future research include the application of our results to commercial QKD implementations; the development of physical Quantum Fuzzing devices, as well as additional strategies for Quantum Fuzzing (especially against QKD state preparation devices); and the continued exploration of vulnerability types in QKD devices and generic exploit methods, in order to provide a more complete map of QKD implementation attacks.

To sum up, in this work we have begun to bridge the gap between practical security

analyses of QKD implementations and the decades-long extensive research in the field of classical cybersecurity. We hope that this research improves the practical security of future QKD products and enhances their usefulness in real-world systems.

Acknowledgements

The work of R.L. was partly supported by the Government of Spain (Severo Ochoa CEX2019-000910-S, FUNQIP, and European Union NextGenerationEU PRTR-C17.I1), Fundació Cellex, Fundació Mir-Puig, Generalitat de Catalunya (CERCA program), and the European Union (Quantum Security Networks Partnership, Grant 101114043). The work of T.M. was partly supported by the Technion’s Helen Diller Quantum Center (Haifa, Israel).

References

- [1] Charles H. Bennett and Gilles Brassard. Quantum cryptography: Public key distribution and coin tossing. In *International Conference on Computers, Systems & Signal Processing*, pages 175–179, 1984.
- [2] Charles H. Bennett. Quantum cryptography using any two nonorthogonal states. *Physical Review Letters*, 68(21):3121–3124, May 1992. doi:[10.1103/PhysRevLett.68.3121](https://doi.org/10.1103/PhysRevLett.68.3121).
- [3] Artur K. Ekert. Quantum cryptography based on Bell’s theorem. *Physical Review Letters*, 67(6), August 1991. doi:[10.1103/PhysRevLett.67.661](https://doi.org/10.1103/PhysRevLett.67.661).
- [4] Damien Stucki, Nicolas Brunner, Nicolas Gisin, Valerio Scarani, and Hugo Zbinden. Fast and simple one-way quantum key distribution. *Applied Physics Letters*, 87(19):194108, November 2005. doi:[10.1063/1.2126792](https://doi.org/10.1063/1.2126792).
- [5] Feihu Xu, Xiongfeng Ma, Qiang Zhang, Hoi-Kwong Lo, and Jian-Wei Pan. Secure quantum key distribution with realistic devices. *Reviews of Modern Physics*, 92(2):025002, May 2020. doi:[10.1103/RevModPhys.92.025002](https://doi.org/10.1103/RevModPhys.92.025002).
- [6] Dominic Mayers. Unconditional security in quantum cryptography. *Journal of the ACM*, 48(3), May 2001. doi:[10.1145/382780.382781](https://doi.org/10.1145/382780.382781).
- [7] Peter W. Shor and John Preskill. Simple proof of security of the BB84 quantum key distribution protocol. *Physical Review Letters*, 85:441–444, July 2000. doi:[10.1103/PhysRevLett.85.441](https://doi.org/10.1103/PhysRevLett.85.441).
- [8] Eli Biham, Michel Boyer, P. Oscar Boykin, Tal Mor, and Vwani Roychowdhury. A proof of the security of quantum key distribution (extended abstract). In *Proceedings of the Thirty-Second Annual ACM Symposium on Theory of Computing*, STOC ’00, pages 715–724, New York, NY, USA, May 2000. Association for Computing Machinery. doi:[10.1145/335305.335406](https://doi.org/10.1145/335305.335406).
- [9] Eli Biham, Michel Boyer, P. Oscar Boykin, Tal Mor, and Vwani Roychowdhury. A proof of the security of quantum key distribution. *Journal of Cryptology*, 19(4):381–439, April 2006. doi:[10.1007/s00145-005-0011-3](https://doi.org/10.1007/s00145-005-0011-3).
- [10] Renato Renner. Security of quantum key distribution. *International Journal of Quantum Information*, 06(01):1–127, February 2008. doi:[10.1142/S0219749908003256](https://doi.org/10.1142/S0219749908003256).
- [11] Michael Ben-Or, Michał Horodecki, Debbie W. Leung, Dominic Mayers, and Jonathan Oppenheim. The universal composable security of quantum key distribution. In *Theory of Cryptography*, Lecture Notes in Computer Science, pages 386–406. Springer, 2005. doi:[10.1007/978-3-540-30576-7_21](https://doi.org/10.1007/978-3-540-30576-7_21).

- [12] Charles H. Bennett, François Bessette, Gilles Brassard, Louis Salvail, and John Smolin. Experimental quantum cryptography. *Journal of Cryptology*, 5(1):3–28, January 1992. doi:[10.1007/BF00191318](https://doi.org/10.1007/BF00191318).
- [13] A. Muller, T. Herzog, B. Huttner, W. Tittel, H. Zbinden, and N. Gisin. “Plug and play” systems for quantum cryptography. *Applied Physics Letters*, 70(7):793–795, February 1997. doi:[10.1063/1.118224](https://doi.org/10.1063/1.118224).
- [14] Damien Stucki, Claudio Barreiro, Sylvain Fasel, Jean-Daniel Gautier, Olivier Gay, Nicolas Gisin, Rob Thew, Yann Thoma, Patrick Trinkler, Fabien Vannel, and Hugo Zbinden. Continuous high speed coherent one-way quantum key distribution. *Optics Express*, 17(16):13326, August 2009. doi:[10.1364/OE.17.013326](https://doi.org/10.1364/OE.17.013326).
- [15] M Peev, C Pacher, R Alléaume, C Barreiro, J Bouda, W Boxleitner, T Debuisschert, E Diamanti, M Dianati, J F Dynes, S Fasel, S Fossier, M Fürst, J-D Gautier, O Gay, N Gisin, P Grangier, A Happe, Y Hasani, M Hentschel, H Hübel, G Humer, T Länger, M Legré, R Lieger, J Lodewyck, T Lorünser, N Lütkenhaus, A Marhold, T Matyus, O Maurhart, L Monat, S Nauerth, J-B Page, A Poppe, E Querasser, G Ribordy, S Robyr, L Salvail, A W Sharpe, A J Shields, D Stucki, M Suda, C Tamas, T Themel, R T Thew, Y Thoma, A Treiber, P Trinkler, R Tualle-Brouri, F Vannel, N Walenta, H Weier, H Weinfurter, I Wimberger, Z L Yuan, H Zbinden, and A Zeilinger. The SECOQC quantum key distribution network in Vienna. *New Journal of Physics*, 11(7):075001, July 2009. doi:[10.1088/1367-2630/11/7/075001](https://doi.org/10.1088/1367-2630/11/7/075001).
- [16] Gilles Brassard, Norbert Lütkenhaus, Tal Mor, and Barry C. Sanders. Limitations on practical quantum cryptography. *Physical Review Letters*, 85(6):1330–1333, August 2000. doi:[10.1103/PhysRevLett.85.1330](https://doi.org/10.1103/PhysRevLett.85.1330).
- [17] Artem Vakhitov, Vadim Makarov, and Dag R. Hjelle. Large pulse attack as a method of conventional optical eavesdropping in quantum cryptography. *Journal of Modern Optics*, 48(13):2023–2038, November 2001. doi:[10.1080/09500340108240904](https://doi.org/10.1080/09500340108240904).
- [18] N. Gisin, S. Fasel, B. Kraus, H. Zbinden, and G. Ribordy. Trojan-horse attacks on quantum-key-distribution systems. *Physical Review A*, 73(2):022320, February 2006. doi:[10.1103/PhysRevA.73.022320](https://doi.org/10.1103/PhysRevA.73.022320).
- [19] Vadim Makarov and Dag R. Hjelle. Faked states attack on quantum cryptosystems. *Journal of Modern Optics*, 52(5):691–705, March 2005. doi:[10.1080/09500340410001730986](https://doi.org/10.1080/09500340410001730986).
- [20] Vadim Makarov and Johannes Skaar. Faked states attack using detector efficiency mismatch on SARG04, phase-time, DPSK, and Ekert protocols. *Quantum Information and Computation*, 8(6 and 7):622–635, July 2008. doi:[10.26421/qic8.6-7-4](https://doi.org/10.26421/qic8.6-7-4).
- [21] Lars Lydersen, Carlos Wiechers, Christoffer Wittmann, Dominique Elser, Johannes Skaar, and Vadim Makarov. Hacking commercial quantum cryptography systems by tailored bright illumination. *Nature Photonics*, 4(10):686–689, October 2010. doi:[10.1038/nphoton.2010.214](https://doi.org/10.1038/nphoton.2010.214).
- [22] Xiao-Ling Pang, Ai-Lin Yang, Chao-Ni Zhang, Jian-Peng Dou, Hang Li, Jun Gao, and Xian-Min Jin. Hacking quantum key distribution via injection locking. *Physical Review Applied*, 13(3), March 2020. doi:[10.1103/physrevapplied.13.034008](https://doi.org/10.1103/physrevapplied.13.034008).
- [23] Bing Qi, Chi-Hang Fred Fung, Hoi-Kwong Lo, and Xiongfeng Ma. Time-shift attack in practical quantum cryptosystems. *Quantum Information and Computation*, 7(1):73–82, January 2007. doi:[10.26421/QIC7.1-2-3](https://doi.org/10.26421/QIC7.1-2-3).

- [24] Michel Boyer, Ran Gelles, and Tal Mor. Attacks on fixed apparatus quantum key distribution schemes. *Physical Review A*, 90(1):012329, July 2014. doi:[10.1103/PhysRevA.90.012329](https://doi.org/10.1103/PhysRevA.90.012329).
- [25] Chris Anley, John Heasman, Felix Lindner, and Gerardo Richarte. *The Shellcoder's Handbook: Discovering and Exploiting Security Holes*. Wiley, 2nd edition, 2007. URL: <https://www.wiley.com/en-us/The+Shellcoder%27s+Handbook%3A+Discovering+and+Exploiting+Security+Holes%2C+2nd+Edition-p-9780470080238>.
- [26] Ron Ross, Victoria Pillitteri, Richard Graubart, Deborah Bodeau, and Rosalie McQuaid. *Developing cyber-resilient systems: a systems security engineering approach*. National Institute of Standards and Technology, December 2021. doi:[10.6028/nist.sp.800-160v2r1](https://doi.org/10.6028/nist.sp.800-160v2r1).
- [27] Ran Gelles and Tal Mor. On the security of interferometric quantum key distribution. In Adrian-Horia Dediu, Carlos Martín-Vide, and Bianca Truthe, editors, *Theory and Practice of Natural Computing*, Lecture Notes in Computer Science, pages 133–146, Berlin, Heidelberg, 2012. Springer. doi:[10.1007/978-3-642-33860-1_12](https://doi.org/10.1007/978-3-642-33860-1_12).
- [28] Ran Gelles and Tal Mor. Reversed space attacks. *arXiv preprint arXiv:1110.6573v2*, May 2016. URL: <https://arxiv.org/abs/1110.6573v2>.
- [29] C Wiechers, L Lydersen, C Wittmann, D Elser, J Skaar, Ch Marquardt, V Makarov, and G Leuchs. After-gate attack on a quantum cryptosystem. *New Journal of Physics*, 13(1):013043, January 2011. doi:[10.1088/1367-2630/13/1/013043](https://doi.org/10.1088/1367-2630/13/1/013043).
- [30] Christoph Marquardt, Ulrich Seyfarth, Sven Bettendorf, Martin Bohmann, Alexander Buchner, Marcos Curty, Dominique Elser, Silas Eul, Tobias Gehring, Nitin Jain, Thomas Klocke, Marie Reinecke, Nico Sieber, Rupert Ursin, Marc Wehling, and Henning Weier. Implementation attacks against QKD systems, 2023. URL: https://www.bsi.bund.de/SharedDocs/Downloads/EN/BSI/Publications/Studies/QKD-Systems/QKD-Systems.pdf?__blob=publicationFile&v=3.
- [31] Vadim Makarov. Controlling passively quenched single photon detectors by bright light. *New Journal of Physics*, 11(6):065003, June 2009. doi:[10.1088/1367-2630/11/6/065003](https://doi.org/10.1088/1367-2630/11/6/065003).
- [32] Rotem Liss and Tal Mor. From practice to theory: The “bright illumination” attack on quantum key distribution systems. In *Theory and Practice of Natural Computing*, Lecture Notes in Computer Science, pages 82–94. Springer International Publishing, 2020. doi:[10.1007/978-3-030-63000-3_7](https://doi.org/10.1007/978-3-030-63000-3_7).
- [33] Zhiliang Yuan, Akira Murakami, Mamko Kujiraoka, Marco Lucamarini, Yoshimichi Tanizawa, Hideaki Sato, Andrew J. Shields, Alan Plews, Ririka Takahashi, Kazuaki Doi, Winci Tam, Andrew W. Sharpe, Alexander R. Dixon, Evan Lavelle, and James F. Dynes. 10-Mb/s quantum key distribution. *Journal of Lightwave Technology*, 36(16):3427–3433, August 2018. doi:[10.1109/jlt.2018.2843136](https://doi.org/10.1109/jlt.2018.2843136).
- [34] Yichen Zhang, Ziyang Chen, Stefano Pirandola, Xiangyu Wang, Chao Zhou, Binjie Chu, Yijia Zhao, Bingjie Xu, Song Yu, and Hong Guo. Long-distance continuous-variable quantum key distribution over 202.81 km of fiber. *Physical Review Letters*, 125(1), June 2020. doi:[10.1103/physrevlett.125.010502](https://doi.org/10.1103/physrevlett.125.010502).
- [35] Jiu-Peng Chen, Chi Zhang, Yang Liu, Cong Jiang, Wei-Jun Zhang, Zhi-Yong Han, Shi-Zhao Ma, Xiao-Long Hu, Yu-Huai Li, Hui Liu, Fei Zhou, Hai-Feng Jiang, Teng-Yun Chen, Hao Li, Li-Xing You, Zhen Wang, Xiang-Bin Wang, Qiang Zhang, and Jian-Wei Pan. Twin-field quantum key distribution over a 511-km optical fibre linking two distant metropolitan areas. *Nature Photonics*, 15(8):570–575, June 2021. doi:[10.1038/s41566-021-00828-5](https://doi.org/10.1038/s41566-021-00828-5).

- [36] Leong-Chuan Kwek, Lin Cao, Wei Luo, Yunxiang Wang, Shihai Sun, Xiangbin Wang, and Ai Qun Liu. Chip-based quantum key distribution. *AAPPS Bulletin*, 31(1), June 2021. doi:[10.1007/s43673-021-00017-0](https://doi.org/10.1007/s43673-021-00017-0).
- [37] Francesco Basso Basset, Mauro Valeri, Emanuele Roccia, Valerio Muredda, Davide Poderini, Julia Neuwirth, Nicolò Spagnolo, Michele B. Rota, Gonzalo Carvacho, Fabio Sciarrino, and Rinaldo Trotta. Quantum key distribution with entangled photons generated on demand by a quantum dot. *Science Advances*, 7(12), March 2021. doi:[10.1126/sciadv.abe6379](https://doi.org/10.1126/sciadv.abe6379).
- [38] Vadim Makarov, Andrey Anisimov, and Johannes Skaar. Effects of detector efficiency mismatch on security of quantum cryptosystems. *Physical Review A*, 74:022313, August 2006. doi:[10.1103/PhysRevA.74.022313](https://doi.org/10.1103/PhysRevA.74.022313).
- [39] Víctor Zapatero, Álvaro Navarrete, and Marcos Curty. Implementation security in quantum key distribution. *Advanced Quantum Technologies*, 8(2):2300380, February 2025. doi:[10.1002/qute.202300380](https://doi.org/10.1002/qute.202300380).
- [40] Michael Reck, Anton Zeilinger, Herbert J. Bernstein, and Philip Bertani. Experimental realization of any discrete unitary operator. *Physical Review Letters*, 73:58–61, July 1994. doi:[10.1103/PhysRevLett.73.58](https://doi.org/10.1103/PhysRevLett.73.58).
- [41] Aleph One. Smashing the stack for fun and profit. *Phrack Magazine*, 7(49), November 1996. Article 14. URL: <http://phrack.org/issues/49/14.html>.
- [42] Barton P. Miller, Lars Fredriksen, and Bryan So. An empirical study of the reliability of unix utilities. *Communications of the ACM*, 33(12):32–44, December 1990. doi:[10.1145/96267.96279](https://doi.org/10.1145/96267.96279).
- [43] Robert C. Seacord. *Secure Coding in C and C++*. Addison-Wesley Professional, 2nd edition, April 2013. URL: <https://insights.sei.cmu.edu/library/secure-coding-in-c-and-c-second-edition/>.
- [44] Pratyusa K. Manadhata and Jeannette M. Wing. An attack surface metric. *IEEE Transactions on Software Engineering*, 37(3):371–386, 2011. doi:[10.1109/TSE.2010.60](https://doi.org/10.1109/TSE.2010.60).
- [45] Hovav Shacham. The geometry of innocent flesh on the bone: Return-into-libc without function calls (on the x86). In *Proceedings of the 14th ACM Conference on Computer and Communications Security (CCS)*, pages 552–561. ACM, 2007. doi:[10.1145/1315245.1315313](https://doi.org/10.1145/1315245.1315313).
- [46] Hovav Shacham, Matthew Page, Ben Pfaff, Eu-Jin Goh, Nagendra Modadugu, and Dan Boneh. On the effectiveness of address space randomization. In *Proceedings of the 11th ACM Conference on Computer and Communications Security (CCS)*, pages 298–307. ACM, 2004. doi:[10.1145/1030083.1030124](https://doi.org/10.1145/1030083.1030124).
- [47] Martín Abadi, Mihai Budiu, Úlfar Erlingsson, and Jay Ligatti. Control-flow integrity. In *Proceedings of the 12th ACM Conference on Computer and Communications Security (CCS)*, pages 340–353. ACM, 2005. doi:[10.1145/1102120.1102165](https://doi.org/10.1145/1102120.1102165).
- [48] Gilles Brassard, Norbert Lütkenhaus, Tal Mor, and Barry C. Sanders. Security aspects of practical quantum cryptography. In Bart Preneel, editor, *Advances in Cryptology — EUROCRYPT 2000*, pages 289–299, Berlin, Heidelberg, 2000. Springer Berlin Heidelberg. doi:[10.1007/3-540-45539-6_20](https://doi.org/10.1007/3-540-45539-6_20).
- [49] Normand J. Beaudry, Tobias Moroder, and Norbert Lütkenhaus. Squashing models for optical measurements in quantum communication. *Physical Review Letters*, 101:093601, August 2008. doi:[10.1103/PhysRevLett.101.093601](https://doi.org/10.1103/PhysRevLett.101.093601).

- [50] Jiyuan Wang, Ming Gao, Yu Jiang, Jianguang Lou, Yue Gao, Dongmei Zhang, and Jianguang Sun. QuanFuzz: Fuzz testing of quantum program. *arXiv preprint arXiv:1810.10310*, 2018. URL: <https://arxiv.org/abs/1810.10310>.
- [51] Daniel Blackwell, Justyna Petke, Yazhuo Cao, and Avner Bensoussan. Fuzzing-based differential testing for quantum simulators. In *International Symposium on Search Based Software Engineering*, pages 63–69. Springer, 2024. doi:10.1007/978-3-031-64573-0_6.
- [52] Xiaoqi Zhao, Haipeng Qu, Jianliang Xu, Xiaohui Li, Wenjie Lv, and Gai-Ge Wang. A systematic review of fuzzing. *Soft Computing*, 28(6):5493–5522, March 2024. doi:10.1007/s00500-023-09306-2.
- [53] Sanoop Mallisery and Yu-Sung Wu. Demystify the fuzzing methods: A comprehensive survey. *ACM Computing Surveys*, 56(3), October 2023. doi:10.1145/3623375.
- [54] Yong-gang Tan, Hua Lu, and Qing-yu Cai. Comment on “quantum key distribution with classical Bob”. *Physical Review Letters*, 102:098901, March 2009. doi:10.1103/PhysRevLett.102.098901.
- [55] D. Gottesman, H.-K. Lo, N. Lutkenhaus, and J. Preskill. Security of quantum key distribution with imperfect devices. In *International Symposium on Information Theory, 2004. ISIT 2004. Proceedings.*, page 136, 2004. doi:10.1109/ISIT.2004.1365172.
- [56] Sebastien Sauge, Lars Lydersen, Andrey Anisimov, Johannes Skaar, and Vadim Makarov. Controlling an actively-quenched single photon detector with bright light. *Optics Express*, 19(23):23590–23600, Nov 2011. doi:10.1364/OE.19.023590.
- [57] Yakir Aharonov, Peter G. Bergmann, and Joel L. Lebowitz. Time symmetry in the quantum process of measurement. *Physical Review*, 134:B1410–B1416, June 1964. doi:10.1103/PhysRev.134.B1410.
- [58] Yakir Aharonov and Lev Vaidman. Properties of a quantum system during the time interval between two measurements. *Physical Review A*, 41:11–20, January 1990. doi:10.1103/PhysRevA.41.11.
- [59] Eli Biham, Bruno Huttner, and Tal Mor. Quantum cryptographic network based on quantum memories. *Physical Review A*, 54(4), October 1996. doi:10.1103/PhysRevA.54.2651.
- [60] Won-Young Hwang and Intaek Lim and Jongwon Park. No-clicking event in the quantum key distribution. *Journal of the Korean Physical Society*, 52(6):1726–1729, June 2008. doi:10.3938/jkps.52.1726.
- [61] Michel Boyer, Dan Kenigsberg, and Tal Mor. Quantum key distribution with classical Bob. *Physical Review Letters*, 99(14), October 2007. doi:10.1103/PhysRevLett.99.140501.
- [62] Paul C. Kocher. Timing attacks on implementations of Diffie-Hellman, RSA, DSS, and other systems. In *Advances in Cryptology — CRYPTO ’96*, pages 104–113. Springer Berlin Heidelberg, 1996. doi:10.1007/3-540-68697-5_9.
- [63] Billy Bob Brumley and Nicola Tuveri. Remote timing attacks are still practical. In Vijay Atluri and Claudia Diaz, editors, *Computer Security – ESORICS 2011*, pages 355–371, Berlin, Heidelberg, 2011. Springer Berlin Heidelberg. doi:10.1007/978-3-642-23822-2_20.
- [64] Dan Boneh, Richard A. DeMillo, and Richard J. Lipton. On the importance of checking cryptographic protocols for faults. In Walter Fumy, editor, *Advances in Cryptology — EUROCRYPT ’97*, pages 37–51, Berlin, Heidelberg, 1997. Springer Berlin Heidelberg. doi:10.1007/3-540-69053-0_4.

- [65] Eli Biham and Adi Shamir. Differential fault analysis of secret key cryptosystems. In Burton S. Kaliski, editor, *Advances in Cryptology — CRYPTO '97*, pages 513–525, Berlin, Heidelberg, 1997. Springer Berlin Heidelberg. doi:[10.1007/bfb0052259](https://doi.org/10.1007/bfb0052259).
- [66] Paul A. Grassi, Michael E. Garcia, and James L. Fenton. Digital identity guidelines. Technical Report NIST SP 800-63-3, National Institute of Standards and Technology, June 2017. Revision 3. doi:[10.6028/NIST.SP.800-63-3](https://doi.org/10.6028/NIST.SP.800-63-3).
- [67] Sebastian Nauerth, Martin Fürst, Tobias Schmitt-Manderbach, Henning Weier, and Harald Weinfurter. Information leakage via side channels in freespace BB84 quantum cryptography. *New Journal of Physics*, 11(6):065001, June 2009. doi:[10.1088/1367-2630/11/6/065001](https://doi.org/10.1088/1367-2630/11/6/065001).
- [68] Lars Lydersen, Carlos Wiechers, Christoffer Wittmann, Dominique Elser, Johannes Skaar, and Vadim Makarov. Thermal blinding of gated detectors in quantum cryptography. *Optics Express*, 18(26):27938–27954, December 2010. doi:[10.1364/OE.18.027938](https://doi.org/10.1364/OE.18.027938).
- [69] Gaëtan Gras, Nigar Sultana, Anqi Huang, Thomas Jennewein, Félix Bussi eres, Vadim Makarov, and Hugo Zbinden. Optical control of single-photon negative-feedback avalanche diode detector. *Journal of Applied Physics*, 127(9), March 2020. doi:[10.1063/1.5140824](https://doi.org/10.1063/1.5140824).
- [70] Binwu Gao, Zhihao Wu, Weixu Shi, Yingwen Liu, Dongyang Wang, Chunlin Yu, Anqi Huang, and Junjie Wu. Ability of strong-pulse illumination to hack self-differencing avalanche photodiode detectors in a high-speed quantum-key-distribution system. *Physical Review A*, 106(3), September 2022. doi:[10.1103/physreva.106.033713](https://doi.org/10.1103/physreva.106.033713).
- [71] Lars Lydersen, Mohsen K Akhlaghi, A Hamed Majedi, Johannes Skaar, and Vadim Makarov. Controlling a superconducting nanowire single-photon detector using tailored bright illumination. *New Journal of Physics*, 13(11):113042, nov 2011. doi:[10.1088/1367-2630/13/11/113042](https://doi.org/10.1088/1367-2630/13/11/113042).
- [72] Poompong Chaiwongkhot, Jiaqiang Zhong, Anqi Huang, Hao Qin, Sheng-cai Shi, and Vadim Makarov. Faking photon number on a transition-edge sensor. *EPJ Quantum Technology*, 9(1), September 2022. doi:[10.1140/epjqt/s40507-022-00141-2](https://doi.org/10.1140/epjqt/s40507-022-00141-2).
- [73] Charles H. Bennett, Gilles Brassard, and N. David Mermin. Quantum cryptography without Bell’s theorem. *Physical Review Letters*, 68(5), February 1992. doi:[10.1103/PhysRevLett.68.557](https://doi.org/10.1103/PhysRevLett.68.557).
- [74] Dominic Mayers and Andrew Yao. Quantum cryptography with imperfect apparatus. In *Proceedings of the 39th Annual Symposium on Foundations of Computer Science*, page 503, USA, 1998. IEEE Computer Society. doi:[10.1109/SFCS.1998.743501](https://doi.org/10.1109/SFCS.1998.743501).
- [75] Ilja Gerhardt, Qin Liu, Ant  a Lamas-Linares, Johannes Skaar, Valerio Scarani, Vadim Makarov, and Christian Kurtsiefer. Experimentally faking the violation of Bell’s inequalities. *Physical Review Letters*, 107(17), October 2011. doi:[10.1103/physrevlett.107.170404](https://doi.org/10.1103/physrevlett.107.170404).
- [76] Girish S. Agarwal. *Quantum Optics*. Cambridge University Press, November 2012. doi:[10.1017/cbo9781139035170](https://doi.org/10.1017/cbo9781139035170).
- [77] Christopher Gerry and Peter Knight. *Introductory Quantum Optics*. Cambridge University Press, Cambridge, UK, 2005. URL: <https://doi.org/10.1017/CB09780511791239>.
- [78] P.D. Townsend. Secure key distribution system based on quantum cryptography. *Electronics Letters*, 30(10):809–811, May 1994. doi:[10.1049/el:19940558](https://doi.org/10.1049/el:19940558).

- [79] Richard J. Hughes, George L. Morgan, and C. Glen Peterson. Quantum key distribution over a 48 km optical fibre network. *Journal of Modern Optics*, 47(2-3):533–547, February 2000. doi:[10.1080/09500340008244058](https://doi.org/10.1080/09500340008244058).
- [80] Tadamasa Kimura, Yoshihiro Nambu, Takaaki Hatanaka, Akihisa Tomita, Hideo Kosaka, and Kazuo Nakamura. Single-photon interference over 150 km transmission using silica-based integrated-optic interferometers for quantum cryptography. *Japanese Journal of Applied Physics*, 43(9A):L1217, September 2004. doi:[10.1143/jjap.43.11217](https://doi.org/10.1143/jjap.43.11217).
- [81] C. Gobby, Z. L. Yuan, and A. J. Shields. Quantum key distribution over 122 km of standard telecom fiber. *Applied Physics Letters*, 84(19):3762–3764, May 2004. doi:[10.1063/1.1738173](https://doi.org/10.1063/1.1738173).
- [82] Z L Yuan, A R Dixon, J F Dynes, A W Sharpe, and A J Shields. Practical gigahertz quantum key distribution based on avalanche photodiodes. *New Journal of Physics*, 11(4):045019, April 2009. doi:[10.1088/1367-2630/11/4/045019](https://doi.org/10.1088/1367-2630/11/4/045019).
- [83] M. Lucamarini, K. A. Patel, J. F. Dynes, B. Fröhlich, A. W. Sharpe, A. R. Dixon, Z. L. Yuan, R. V. Penty, and A. J. Shields. Efficient decoy-state quantum key distribution with quantified security. *Optics Express*, 21(21):24550, October 2013. doi:[10.1364/OE.21.024550](https://doi.org/10.1364/OE.21.024550).
- [84] Nicolas Gisin, Grégoire Ribordy, Wolfgang Tittel, and Hugo Zbinden. Quantum cryptography. *Reviews of Modern Physics*, 74(1):145–195, March 2002. doi:[10.1103/revmodphys.74.145](https://doi.org/10.1103/revmodphys.74.145).
- [85] Zachary D. Walton, Ayman F. Abouraddy, Alexander V. Sergienko, Bahaa E. A. Saleh, and Malvin C. Teich. Decoherence-free subspaces in quantum key distribution. *Physical Review Letters*, 91:087901, August 2003. doi:[10.1103/PhysRevLett.91.087901](https://doi.org/10.1103/PhysRevLett.91.087901).
- [86] Yoshihiro Nambu, Takaaki Hatanaka, and Kazuo Nakamura. BB84 quantum key distribution system based on silica-based planar lightwave circuits. *Japanese Journal of Applied Physics*, 43(8B):L1109, July 2004. doi:[10.1143/jjap.43.11109](https://doi.org/10.1143/jjap.43.11109).
- [87] Gregg Jaeger. Entangled states in quantum key distribution. In *AIP Conference Proceedings*, volume 810, pages 161–167. AIP, 2006. doi:[10.1063/1.2158719](https://doi.org/10.1063/1.2158719).
- [88] M. Sasaki, M. Fujiwara, H. Ishizuka, W. Klaus, K. Wakui, M. Takeoka, S. Miki, T. Yamashita, Z. Wang, A. Tanaka, K. Yoshino, Y. Nambu, S. Takahashi, A. Tajima, A. Tomita, T. Domeki, T. Hasegawa, Y. Sakai, H. Kobayashi, T. Asai, K. Shimizu, T. Tokura, T. Tsurumaru, M. Matsui, T. Honjo, K. Tamaki, H. Takesue, Y. Tokura, J. F. Dynes, A. R. Dixon, A. W. Sharpe, Z. L. Yuan, A. J. Shields, S. Uchikoga, M. Legré, S. Robyr, P. Trinkler, L. Monat, J.-B. Page, G. Ribordy, A. Poppe, A. Allacher, O. Maurhart, T. Länger, M. Peev, and A. Zeilinger. Field test of quantum key distribution in the Tokyo QKD network. *Optics Express*, 19(November):10387, May 2011. doi:[10.1364/OE.19.010387](https://doi.org/10.1364/OE.19.010387).
- [89] Alberto Boaron, Boris Korzh, Raphael Houlmann, Gianluca Boso, Davide Rusca, Stuart Gray, Ming-Jun Li, Daniel Nolan, Anthony Martin, and Hugo Zbinden. Simple 2.5GHz time-bin quantum key distribution. *Applied Physics Letters*, 112(17), April 2018. doi:[10.1063/1.5027030](https://doi.org/10.1063/1.5027030).
- [90] Fabian Beutel, Helge Gehring, Martin A. Wolff, Carsten Schuck, and Wolfram Pernice. Detector-integrated on-chip QKD receiver for GHz clock rates. *npj Quantum Information*, 7(1):40, February 2021. doi:[10.1038/s41534-021-00373-7](https://doi.org/10.1038/s41534-021-00373-7).
- [91] Hoi-Kwong Lo and H. F. Chau. Unconditional security of quantum key distribution over arbitrarily long distances. *Science*, 283(5410):2050–2056, 1999. doi:[10.1126/science.283.5410.2050](https://doi.org/10.1126/science.283.5410.2050).

- [92] Hoi-Kwong Lo. Proof of unconditional security of six-state quantum key distribution scheme. *arXiv preprint arXiv:quant-ph/0102138*, 2001. URL: <https://arxiv.org/abs/quant-ph/0102138>.

A Application of Linear Optical Devices on Photonic States

In this appendix, we discuss physical implementations of QKD schemes using photons. We first describe *Fock-space notations*, which are easier to use when considering photon-implemented qubits. We then describe the unitary transformation that describes various optical devices commonly used in contemporary QKD implementations, such as beam splitters, phase shifters, and interferometers. We explain the quantum state of a photon (or more generally, a pulse of photons) passing through these optical devices.

Symmetric Beam Splitter

A beam splitter has two input arms (modes 1 and 2) and two output arms (modes 3 and 4), see Figure 3. Given that the Beam Splitter is symmetric, Each entering photon has equal amplitude for transmittance and reflection; The transmitted part keeps the same phase as the incoming photon, while the reflected part gets an extra phase of $e^{i\pi/2}$. Specifically, $|10\rangle_{1,2}^F \rightarrow \frac{1}{\sqrt{2}}(|10\rangle_{3,4}^F + i|01\rangle_{3,4}^F)$ and $|01\rangle_{1,2}^F \rightarrow \frac{1}{\sqrt{2}}(i|10\rangle_{3,4}^F + |01\rangle_{3,4}^F)$. Thus, for a single photon state in a general superposition between the two input arms, the transformation is given by

$$\alpha|10\rangle_{1,2}^F + \beta|01\rangle_{1,2}^F \mapsto \frac{\alpha + i\beta}{\sqrt{2}}|10\rangle_{3,4}^F + \frac{i\alpha + \beta}{\sqrt{2}}|01\rangle_{3,4}^F. \quad (8)$$

It is important to note that when a single mode (carrying a single photon) enters a beam splitter from one arm, and nothing (namely, vacuum) enters the other arm (say, $\alpha = 1; \beta = 0$), there are still two input modes and two output modes. This means that the other (vacuum) entry must be considered as an additional mode — an ancilla carrying no photons.

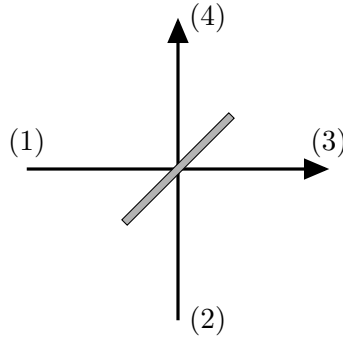


Figure 3: A symmetric beam splitter with two input modes (1) and (2) and two output modes (3) and (4).

Action on a High-Photon-Number Pulse

According to [76], the result of a symmetric beam splitter on a pulse with n photons, denoted as $|n, 0\rangle_{1,2}$, is given by:

$$|\psi_{\text{out}}\rangle = \frac{1}{\sqrt{2^n}} \sum_{k=0}^n \sqrt{\binom{n}{k}} |k, n-k\rangle_{3,4}. \quad (9)$$

Phase Shifter

A controlled phase shifter P_ϕ performs a phase shift on the input state by a given phase ϕ , i.e. $P_\phi(|n\rangle^F) = e^{i \cdot n \cdot \phi} |n\rangle^F$, see [77].

Mach-Zehnder Interferometer

A Mach-Zehnder interferometer (Figure 6) is a device composed of two beam splitters (BS) with one short path, one long path, and a controlled phase shifter P_ϕ , that is placed at the long arm of the interferometer.

We will now describe the operation of the interferometer on input states similar to those used in the example protocol in Section 5.3, under the more generic and physically accurate Fock-space notations (Section 2.2).

In each transmission, a superposition of two (time) modes enters the interferometer and result in a superposition of 6 modes (Figure 6). The input modes are separated with a time difference of ΔT seconds, that is, the first mode arrives at time t'_0 , and the second at $t'_1 = t'_0 + \Delta T$. The first pulse travels through the short arm in T_{short} seconds, and through the long arm in $T_{\text{long}} = T_{\text{short}} + \Delta T$ seconds, where the time difference between the two arms is exactly the time difference ΔT between the two incoming modes. Due to traveling through both arms, the first mode yields outgoing pulses both at time $t_0 \equiv t'_0 + T_{\text{short}}$ and at $t_1 \equiv t'_0 + T_{\text{long}} = t'_0 + T_{\text{short}} + \Delta T = t_0 + \Delta T$.

When the second pulse enters the interferometer, it also travels through both arms. Intuitively, the part of the t'_1 mode that travels through the short arm interferes with the part of the t'_0 mode that travels through the long arm, and the output exits the interferometer at t_1 . The part of the second pulse that travels through the long arm exits the interferometer at time $t_2 = t_1 + \Delta T$. As a result, there are six different possible modes at the two output arms, three in each direction, with the two middle pulses determined by the interference between the two pulses arriving into Bob's lab. We shall now show the mathematical formulation behind these statements.

Evolution of a Single-Time-Bin Photon Through a Mach-Zehnder Interferometer

When a single mode, carrying one or more photons, enters the interferometer, three ancillas in a vacuum state are added by the interferometric setup (see Figure 4). As mentioned above, the mode that enters the interferometer at time t'_0 , yields two modes at time t_0 , and two modes at time t_1 . These four output modes are: times t_0, t_1 at the 's' (straight) arm of the interferometer, and times t_0, t_1 at the 'd' (down) arm of the interferometer. A basis state of this Fock-space can be written as $|n_{s_0}, n_{s_1}, n_{d_0}, n_{d_1}\rangle^F$.

Assume that a single photon enters the interferometer at time t'_0 . Using the above notations, the interferometer's transformation is given by

$$|1\rangle_{t'_0}^F |000\rangle^F \mapsto (|1000\rangle^F - e^{i\phi} |0100\rangle^F + i |0010\rangle^F + i e^{i\phi} |0001\rangle^F) / 2. \quad (10)$$

Note the three vacuum ancillas that were added. Also, note that a pulse which is sent at a different time (say, t'_1 , or t'_{-1} , etc.) results in the same output state, with appropriate delays. That is, a pulse entering the interferometer at time t'_i results in the state $(|1000\rangle^F - e^{i\phi} |0100\rangle^F + i |0010\rangle^F + i e^{i\phi} |0001\rangle^F) / 2$ in a Fock-space with basis states $|n_{s_i}, n_{s_{i+1}}, n_{d_i}, n_{d_{i+1}}\rangle^F$.

Using the more standard notation of $\{|t'_i\rangle\}$ input states and $\{|s_i\rangle, |d_i\rangle\}$ output states used in the rest of the paper, Eq. (10) is given by

$$|t'_i\rangle \mapsto (|s_i\rangle + i |d_i\rangle - e^{i\phi} |s_{i+1}\rangle + i e^{i\phi} |d_{i+1}\rangle) / 2. \quad (11)$$

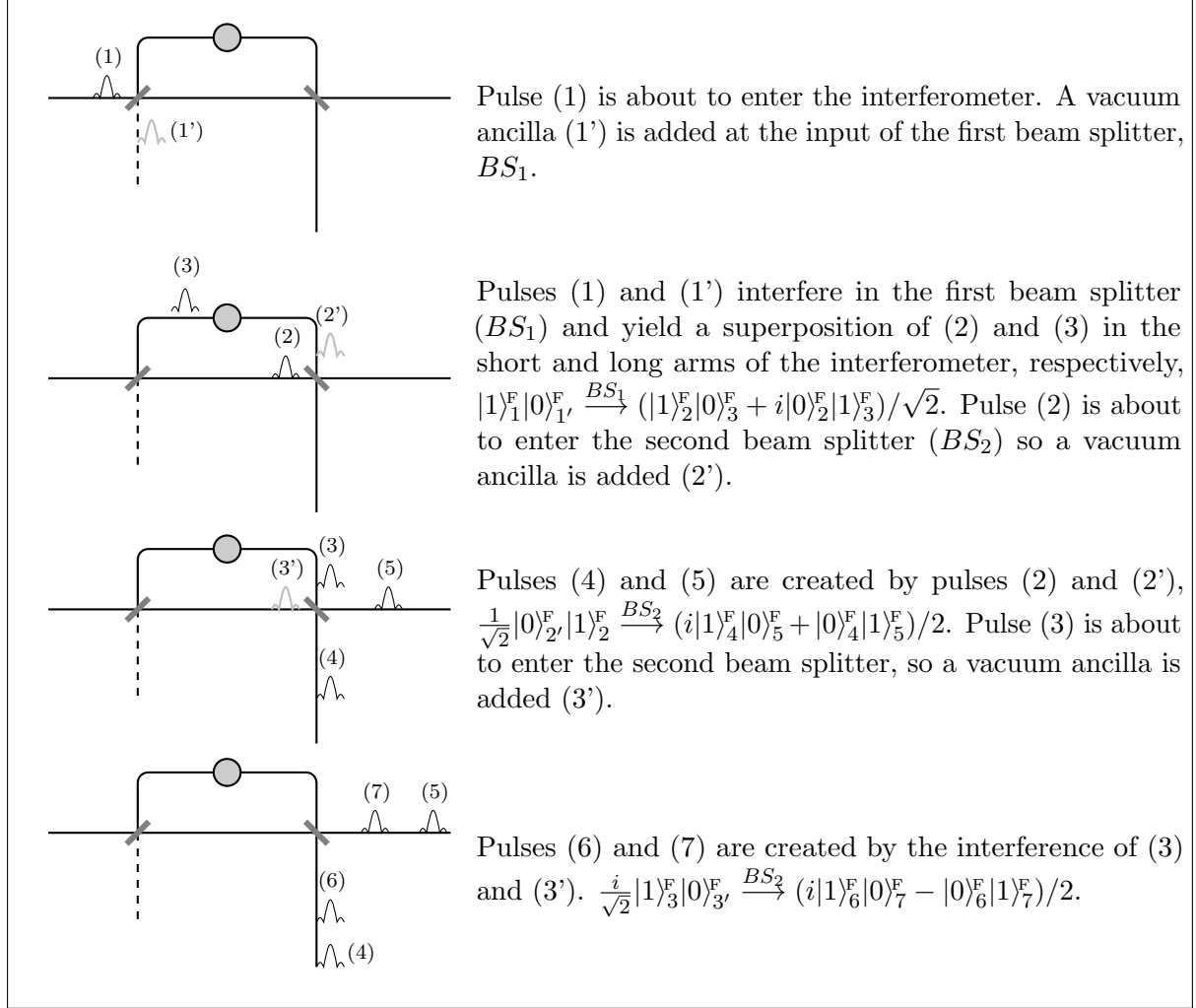


Figure 4: Evolution in time of a single photon pulse through the interferometer with $\phi = 0$, $|1000\rangle_{1,1',2',3'}^F \rightarrow \frac{1}{2}(|1000\rangle^F - |0100\rangle^F + i|0010\rangle^F + i|0001\rangle^F)_{5,7,4,6}$. The output state is denoted by modes $|n_{s_0}, n_{s_1}, n_{d_0}, n_{d_1}\rangle^F$ that correspond to modes (5), (7), (4), and (6), respectively.

Evolution of Photon in Time-Bin Superposition Through Mach-Zehnder Interferometer

We are now ready to consider the setup of Figure 6 and two input modes, t'_0 and t'_1 , that enter the interferometer one after the other, with exactly the same time difference ΔT as the interferometer's arms. As a result of this precise timing, the two modes are transformed into a superposition of only six modes (instead of eight modes) at the outputs (see Figure 5). Four (vacuum state) ancillas are added during the process and the resulting six modes are t_0, t_1, t_2 at the 's' arm and the 'd' arm of the interferometer. A basis state of this Fock-space is, therefore, $|n_{s_0}, n_{s_1}, n_{s_2}, n_{d_0}, n_{d_1}, n_{d_2}\rangle^F$. If exactly one photon enters the interferometer, we can use Eq. (10) to obtain

$$\begin{aligned} |1\rangle_{t'_0}^F |0\rangle_{t'_1}^F |0000\rangle^F &\mapsto (|100000\rangle^F - e^{i\phi}|010000\rangle^F + i|000100\rangle^F + ie^{i\phi}|000010\rangle^F) / 2 \\ |0\rangle_{t'_0}^F |1\rangle_{t'_1}^F |0000\rangle^F &\mapsto (|010000\rangle^F - e^{i\phi}|001000\rangle^F + i|000010\rangle^F + ie^{i\phi}|000001\rangle^F) / 2 \end{aligned} \quad (12)$$

Recall that $|0\rangle = |10\rangle_{t'_0 t'_1}^F$ and $|1\rangle = |01\rangle_{t'_0 t'_1}^F$. It follows that an arbitrary qubit is transformed as

$$\begin{aligned} (\alpha|10\rangle^F + \beta|01\rangle^F) |0000\rangle^F &\longrightarrow \left(\frac{\alpha}{2}|100000\rangle^F + \frac{\beta - \alpha e^{i\phi}}{2}|010000\rangle^F - \frac{\beta e^{i\phi}}{2}|001000\rangle^F \right. \\ &\quad \left. + \frac{i\alpha}{2}|000100\rangle^F + \frac{i(\alpha e^{i\phi} + \beta)}{2}|000010\rangle^F + \frac{i\beta e^{i\phi}}{2}|000001\rangle^F \right). \end{aligned} \quad (13)$$

Reversal of Single Photon Through Mach-Zehnder Interferometer

In our work, we sometimes wish to see the time-reversed operation of a device on a certain measured state, in order to see which states affect it and in which way. We will now perform this analysis for the Mach-Zehnder interferometer.

While the inversion of a unitary transformation is not complicated, it requires two things: a characterization of the relevant Hilbert space, and a characterization of its action on all basis states of that space.

Let U denote the unitary action that the interferometer performs. Let us denote the non-blocked and blocked input arms (a) and (b) respectively, and let us denote the "straight" and "down" output arms (s) and (d) respectively.

While a pulse can arrive at the interferometer at any instance of time (which is continuous), we know that pulses only interfere with each other if their time difference is equal to the time difference of the interferometer's two paths. Thus, we define some instance of time as $t = 0$, and consider all times $\{t \cdot \Delta \mid t \in \mathbb{Z}\}$, where Δ is the interferometer's time difference.

The input space is thus:

$$\text{span}\{|a_t\rangle, |b_t\rangle \mid t \in \mathbb{Z}\}, \quad (14)$$

and the output space is

$$\text{span}\{|s_t\rangle, |d_t\rangle \mid t \in \mathbb{Z}\}, \quad (15)$$

while we have already shown that the evolution for $|a_t\rangle$ is given by:

$$U|a_t\rangle = \left(|s_t\rangle + i|d_t\rangle - e^{i\phi}|s_{t+1}\rangle + ie^{i\phi}|d_{t+1}\rangle \right) / 2. \quad (16)$$

We now need to analyze the evolution of a pulse from the *blocked* arm, as a time-reversed pulse from one of the output arms could quite possibly reach it.

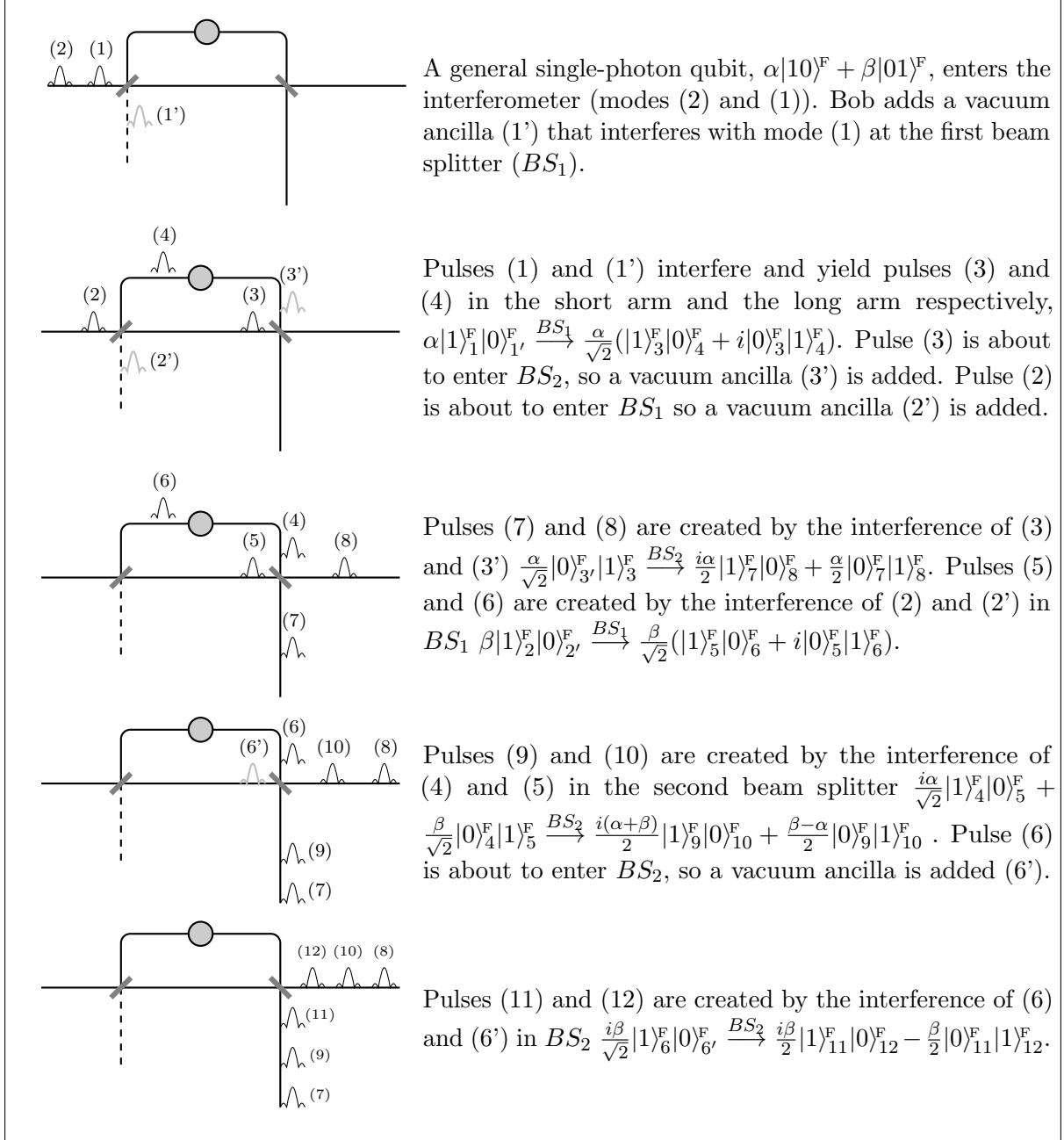


Figure 5: Evolution in time of two modes through the interferometer with $\phi = 0$, $(\alpha|1\rangle_1^F|0\rangle_2^F + \beta|0\rangle_1^F|1\rangle_2^F)|0000\rangle_{1',2',3',6'}^F \rightarrow (\frac{\alpha}{2}|100000\rangle^F + \frac{\beta-\alpha}{2}|010000\rangle^F - \frac{\beta}{2}|001000\rangle^F + \frac{i\alpha}{2}|000100\rangle^F + \frac{i(\alpha+\beta)}{2}|000010\rangle^F + \frac{i\beta}{2}|000001\rangle^F)_{8,10,12,7,9,11}$. The output state is denoted by modes $|n_{s_0}, n_{s_1}, n_{s_2}, n_{d_0}, n_{d_1}, n_{d_2}\rangle^F$.

$$\begin{aligned}
|b_t\rangle & \xrightarrow{\text{beam splitter}} (i|\text{short}_t\rangle + |\text{long}_t\rangle) / \sqrt{2} \\
& \xrightarrow{\text{phase} + \text{delay}} (i|\text{short}_t\rangle + e^{i\phi}|\text{long}_{t+1}\rangle) / \sqrt{2} \\
& \xrightarrow{\text{beam splitter}} (i|s_t\rangle - |d_t\rangle + ie^{i\phi}|s_{t+1}\rangle + e^{i\phi}|d_{t+1}\rangle) / 2.
\end{aligned} \tag{17}$$

Thus, U can be written in matrix form from $(|a_{-1}\rangle, |b_{-1}\rangle, |a_0\rangle, |b_0\rangle, |a_1\rangle, |b_1\rangle, \dots)$ to $(|s_{-1}\rangle, |d_{-1}\rangle, |s_0\rangle, |d_0\rangle, |s_1\rangle, |d_1\rangle, \dots)$ as:

$$U = \frac{1}{2} \begin{pmatrix} 1 & i & 0 & 0 & \dots \\ i & -1 & 0 & 0 & \\ -e^{i\phi} & ie^{i\phi} & 1 & i & \\ ie^{i\phi} & e^{i\phi} & i & -1 & \\ 0 & 0 & -e^{i\phi} & ie^{i\phi} & \\ 0 & 0 & ie^{i\phi} & e^{i\phi} & \\ \vdots & & & & \end{pmatrix}. \tag{18}$$

By inverting the matrix, we get:

$$U^{-1} = U^\dagger = \frac{1}{2} \begin{pmatrix} 1 & -i & -e^{-i\phi} & -ie^{-i\phi} & 0 & 0 & \dots \\ -i & -1 & -ie^{-i\phi} & e^{-i\phi} & 0 & 0 & \\ 0 & 0 & 1 & -i & -e^{-i\phi} & -ie^{-i\phi} & \\ 0 & 0 & -i & -1 & -ie^{-i\phi} & e^{-i\phi} & \\ \vdots & & & & & & \end{pmatrix}. \tag{19}$$

Finally, the formula form for each basis element is given by:

$$\begin{aligned}
U^\dagger|s_t\rangle &= -e^{-i\phi}|a_{t-1}\rangle - ie^{-i\phi}|b_{t-1}\rangle + |a_t\rangle - i|b_t\rangle, \\
U^\dagger|d_t\rangle &= -ie^{-i\phi}|a_{t-1}\rangle + e^{-i\phi}|b_{t-1}\rangle - i|a_t\rangle - |b_t\rangle.
\end{aligned} \tag{20}$$

B Example: Insecurity of Interferometric BB84

In this appendix, we show how to employ the Reversed-Space method on an interferometric BB84 scheme to find the attack described in Section 5.3. In interferometric BB84 schemes, two possible times and a single photon are used to encode a qubit. One basis can be defined by the photon entering at one time or the other, while the other basis is comprised of a superposition of the two times with different phase values. When only states that use both times in a superposition are used, the scheme is called *time-multiplexed, phase-encoded*. Such schemes were initially suggested by [12] and implemented by Townsend [78] and many others (e.g., [79, 80, 81, 82, 83, 33], see as well [84, 5]. Encoding and multiplexing methods are further discussed in Section 8).

In order to produce and measure such superpositioned pulses, it is common to use *interferometers* (see below and Appendix A). Yet, once a protocol is implemented via photons and interferometers, two immediate reasons cause an enlargement of the quantum space in use:⁵ first, interferometers inherently introduce a higher-dimension space; and second, having pulses with zero photons, or more than one photon, implies a higher dimension as well.

In this subsection, we demonstrate a Reversed-Space Attack on an interferometric BB84 implementation. The attack we define here exposes a vulnerability inherent to a large class of implementations, and is *directly applicable* to the implementations in [85, 86, 87] and the NICT-NEC implementation in [88].

⁵There are other possible causes for space enlargement. For instance, the shape of the pulse (in the frequency domain and/or the time domain) is not generated by Alice or measured by Bob in an ideal way, and this opens another source space enlargement.

Our focus in this subsection is on a single physical apparatus. Note that not all interferometric QKD implementations are insecure in this fashion [28], but other implementation methods should still be analyzed [89, 90].

We begin by describing the protocol implementation and the setup Bob uses.

B.1 Interferometric Implementation of BB84

Consider a BB84 implementation which uses two time-separated modes (pulses). For every transmission, the first mode arrives to Bob's lab at time t'_0 , and the second mode at $t'_1 = t'_0 + \Delta T$. We denote these pulses as $|t'_0\rangle$ and $|t'_1\rangle$ respectively. The users use the Hadamard and computational bases, so that an ideal Alice sends one of the following four states,

$$\begin{aligned} |0\rangle_A &\equiv |t'_0\rangle & |+\rangle_A &\equiv (|t'_0\rangle + |t'_1\rangle) / \sqrt{2} \\ |1\rangle_A &\equiv |t'_1\rangle & |-\rangle_A &\equiv (|t'_0\rangle - |t'_1\rangle) / \sqrt{2}. \end{aligned}$$

Bob measures the qubit using a Mach-Zehnder interferometer, which is a device composed of two beam splitters (BS) with one short path, one long path, and a controlled phase shifter P_ϕ , that is placed at the long arm of the interferometer. (See Appendix A for a mode details on linear-optics devices, and analysis of their operation on photonic states). The length difference between the two arms is determined by ΔT : when the first pulse travels through the long arm, and the second through the short arm, they arrive together at the output. Due to that exact timing of the pulses, each incoming qubit is transformed into a superposition of 6 possible modes: 3 time modes (t_0, t_1, t_2) at the straight (s) output arm of the interferometer, and 3 modes at the down (d) output arm; see Figure 6.

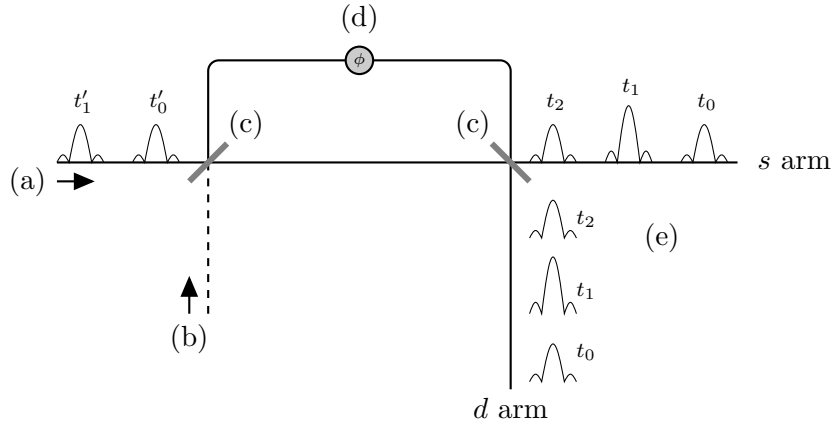


Figure 6: A Mach-Zehnder interferometer. (a) An input qubit. The time-difference between the two incoming modes is identical to the difference between the two arms; (b) a vacuum state entering the second (blocked) arm; (c) beam splitters; (d) phase shifter P_ϕ ; (e) six output modes.

For the sake of simplicity we denote these modes as $s_0, s_1, s_2, d_0, d_1, d_2$, and since we only consider pulses with zero or one photon, we can use the states, $|s_0\rangle, |d_0\rangle$, etc.⁶, along with the vacuum state $|V\rangle$ (a pulse that contains no photons in any of the modes).

The interferometer evolves these states according to $|V\rangle \mapsto |V\rangle_B$ and

$$\begin{aligned} |t'_0\rangle &\mapsto (|s_0\rangle_B - e^{i\phi}|s_1\rangle_B + i|d_0\rangle_B + ie^{i\phi}|d_1\rangle_B)/2 \\ |t'_1\rangle &\mapsto (|s_1\rangle_B - e^{i\phi}|s_2\rangle_B + i|d_1\rangle_B + ie^{i\phi}|d_2\rangle_B)/2. \end{aligned} \tag{21}$$

⁶Using the Fock-space notations (Section 2.2) and the description of interferometers in Appendix A, a basis state in Bob's space is $|n_{s_0}, n_{s_1}, n_{s_2}, n_{d_0}, n_{d_1}, n_{d_2}\rangle^F$, and we define $|100000\rangle^F \equiv |s_0\rangle$; $|010000\rangle^F \equiv |s_1\rangle$; $|001000\rangle^F \equiv |s_2\rangle$; $|000100\rangle^F \equiv |d_0\rangle$; $|000010\rangle^F \equiv |d_1\rangle$; $|000001\rangle^F \equiv |d_2\rangle$, and the vacuum state $|000000\rangle^F \equiv |V\rangle$.

In our example, Bob fixes the phase ϕ to 0. Thus, Alice's qubit evolves in the interferometer as

$$\begin{aligned}
|0\rangle_A &\mapsto (|s_0\rangle_B - |s_1\rangle_B + i|d_0\rangle_B + i|d_1\rangle_B)/2 \\
|1\rangle_A &\mapsto (|s_1\rangle_B - |s_2\rangle_B + i|d_1\rangle_B + i|d_2\rangle_B)/2 \\
|+\rangle_A &\mapsto (|s_0\rangle_B - |s_2\rangle_B + i|d_0\rangle_B + 2i|d_1\rangle_B + i|d_2\rangle_B)/\sqrt{8} \\
|-\rangle_A &\mapsto (|s_0\rangle_B - 2|s_1\rangle_B + |s_2\rangle_B + i|d_0\rangle_B - i|d_2\rangle_B)/\sqrt{8}.
\end{aligned} \tag{22}$$

In order to measure the Hadamard basis, Bob opens his detectors at time t_1 at both arms. A click at the “down” direction (i.e., measuring the state $|d_1\rangle$) means the bit-value 0, while a click at the “straight” direction ($|s_1\rangle$) means 1. The other modes are considered as a loss (namely, they are not measured) since they do not reveal the value of the original qubit.

Similarly, in order to measure in the computational basis, Bob need not measure time t_1 as it does not reveal the value of the original bit. Bob may open his detector in times t_0, t_2 (on both hands) where the former implies measurement of the bit 0 and the latter implies measurement of the bit 1.

B.2 Identifying the Reversed Space of the Interferometric Setup

We now follow the framework defined in the last subsections and specify Bob's operation and the space he measures, in two simple cases. We then derive the corresponding reversed space that applies in each setting.

Example: when Bob measures two modes. Assume that Bob only measures the two modes that correspond to time t_1 , namely, $|s_1\rangle$ and $|d_1\rangle$.⁷

Thus, the space Bob measures, \mathcal{H}^B , is spanned by $B = \{|V\rangle, |s_1\rangle, |d_1\rangle\}$. We can reverse each mode by evolving it backwards in time through the interferometer. As shown in Appendix A, a reversal of a single mode through the interferometer is given by

$$\begin{aligned}
|s_n\rangle &\mapsto (|a_n\rangle - e^{-i\phi}|a_{n-1}\rangle - i|b_n\rangle - ie^{-i\phi}|b_{n-1}\rangle)/2 \\
|d_n\rangle &\mapsto (-i|a_n\rangle - ie^{-i\phi}|a_{n-1}\rangle - |b_n\rangle + e^{-i\phi}|b_{n-1}\rangle)/2.
\end{aligned} \tag{23}$$

Where $|a_n\rangle$ is a pulse in the input arm at time n , and $|b_n\rangle$ is a pulse in the blocked arm at time n . The derivation of the formula is given in Appendix A.

Reversing $|s_1\rangle$ and $|d_1\rangle$ and then “tracing out” the blocked ancillary system (the ‘ b ’ arm) implies that \mathcal{H}^P must include at least the span of $\{|V\rangle, |t'_1\rangle, |t'_0\rangle\}$.

Example: when Bob measures six modes. Now suppose that Bob measures time-bins t_0, t_1, t_2 , so his measured space \mathcal{H}^B is the span of $\{|V\rangle, |d_0\rangle, |d_1\rangle, |d_2\rangle, |s_0\rangle, |s_1\rangle, |s_2\rangle\}$. Again using the reversed transformation in Eq. (23), we get that the reversed space \mathcal{H}^P is much larger than \mathcal{H}^A : it is the space that allows the photon to be in any superposition of time modes t'_{-1} to t'_2 . This means that the analysis needs only focus on the space spanned by $\{|V\rangle, |t'_{-1}\rangle, |t'_0\rangle, |t'_1\rangle, |t'_2\rangle\}$.

B.3 Attack on BB84 Using the Hadamard and Computational Bases: When Bob Measures Six Modes

We will now analyze the interferometric setting described in Section B.1. After defining the interesting spaces for this setting (as shown in the example above), we now try to find oblivious

⁷This setting happens, for instance, when the BB84 protocol is run using the Hadamard and y bases.

attacks, using the formalization of Section 5.2.3. First note that Bob's unitary, U_B , is the same for both the computational and the Hadamard bases, $\beta^C = \beta^H$, and is characterized by

$$\beta^H_{k=\{t'_{-1}, t'_0, t'_1, t'_2\}, j=\{s_0, s_1, s_2, d_0, d_1, d_2\}} = \frac{1}{2} \begin{pmatrix} -1 & 0 & 0 & i & 0 & 0 \\ 1 & -1 & 0 & i & i & 0 \\ 0 & 1 & -1 & 0 & i & i \\ 0 & 0 & 1 & 0 & 0 & i \end{pmatrix},$$

which is immediately given by extending Eq. (21) with $\phi = 0$ to times t'_{-1} and t'_2 .

Denote with $B = \{|V\rangle, |d_0\rangle, |d_1\rangle, |d_2\rangle, |s_0\rangle, |s_1\rangle, |s_2\rangle\}$ a basis of Bob's measured space \mathcal{H}^B . When Bob measures in the Hadamard basis, he interprets his measurement in the following way, $J_0 = \{|d_1\rangle\}$; $J_1 = \{|s_1\rangle\}$; $J_{\text{loss}} = B \setminus (J_0 \cup J_1)$; and $J_{\text{invalid}} = \emptyset$.⁸ Consider the case where Alice sends $|+\rangle$, namely, $\alpha_{t'_0} = \alpha_{t'_1} = \frac{1}{\sqrt{2}}$. An error occurs if Bob measures $|s_1\rangle$, $J_{\text{error}} = \{|s_1\rangle\}$, and by Observation 1, our attack is required to satisfy

$$-\frac{1}{2\sqrt{2}}(\epsilon_{t'_0, t'_0} |E_{t'_0, t'_0}\rangle_E + \epsilon_{t'_1, t'_0} |E_{t'_1, t'_0}\rangle_E) + \frac{1}{2\sqrt{2}}(\epsilon_{t'_0, t'_1} |E_{t'_0, t'_1}\rangle_E + \epsilon_{t'_1, t'_1} |E_{t'_1, t'_1}\rangle_E) = 0. \quad (24)$$

Similarly, when Alice sends $|-\rangle$ an error happens when Bob measures $J_{\text{error}} = \{|d_1\rangle\}$, and thus we require that

$$\frac{i}{2\sqrt{2}}(\epsilon_{t'_0, t'_0} |E_{t'_0, t'_0}\rangle_E - \epsilon_{t'_1, t'_0} |E_{t'_1, t'_0}\rangle_E) + \frac{i}{2\sqrt{2}}(\epsilon_{t'_0, t'_1} |E_{t'_0, t'_1}\rangle_E - \epsilon_{t'_1, t'_1} |E_{t'_1, t'_1}\rangle_E) = 0. \quad (25)$$

As for the computational basis, Bob interprets his outcome according to $J_0 = \{|d_0\rangle, |s_0\rangle\}$, $J_1 = \{|d_2\rangle, |s_2\rangle\}$, $J_{\text{invalid}} = \emptyset$, and $J_{\text{loss}} = B \setminus (J_0 \cup J_1)$. Following Observation 1, an attack U_E which causes no errors is required to satisfy

$$i\epsilon_{t'_0, t'_1} |E_{t'_0, t'_1}\rangle + i\epsilon_{t'_0, t'_2} |E_{t'_0, t'_2}\rangle = 0, \quad -\epsilon_{t'_0, t'_1} |E_{t'_0, t'_1}\rangle + \epsilon_{t'_0, t'_2} |E_{t'_0, t'_2}\rangle = 0, \quad (26)$$

corresponding to the case where Alice sends $|0\rangle$, i.e. $\alpha_{t'_0} = 1$, $\alpha_{t'_1} = 0$, and $J_{\text{error}} = \{|d_2\rangle, |s_2\rangle\}$, as well as

$$i\epsilon_{t'_1, t'_{-1}} |E_{t'_1, t'_{-1}}\rangle + i\epsilon_{t'_1, t'_0} |E_{t'_1, t'_0}\rangle = 0, \quad -\epsilon_{t'_1, t'_{-1}} |E_{t'_1, t'_{-1}}\rangle + \epsilon_{t'_1, t'_0} |E_{t'_1, t'_0}\rangle = 0, \quad (27)$$

corresponding the case where Alice sends $|1\rangle$, i.e. $\alpha_{t'_0} = 0$, $\alpha_{t'_1} = 1$, and $J_{\text{error}} = \{|d_0\rangle, |s_0\rangle\}$. This leads to the constraints $\epsilon_{t'_0, t'_1} = \epsilon_{t'_0, t'_2} = 0$ and $\epsilon_{t'_1, t'_{-1}} = \epsilon_{t'_1, t'_0} = 0$.

Combining all the above requirements yields that the only possible attacks are of the form

$$\begin{aligned} |0\rangle_E |0\rangle_A &\xrightarrow{U_E} p|\phi\rangle_E |t'_0\rangle_P + p_1|\phi_1\rangle |t'_{-1}\rangle_P + p_2|\psi_0\rangle_E |V\rangle_P, \\ |0\rangle_E |1\rangle_A &\xrightarrow{U_E} p|\phi\rangle_E |t'_1\rangle_P + p_3|\phi_2\rangle |t'_2\rangle_P + p_4|\psi_1\rangle_E |V\rangle_P, \end{aligned} \quad (28)$$

with $|p|^2 + |p_1|^2 + |p_2|^2 = |p|^2 + |p_3|^2 + |p_4|^2 = 1$. Using Eq. (28) it is easy to devise an attack and demonstrate that the protocol is completely insecure in the sense that there exists an attack that leaks information without causing any errors. For instance, let

$$|0\rangle_E |0\rangle_A \xrightarrow{U_E} |E_1\rangle_E |t'_{-1}\rangle_P, \quad |0\rangle_E |1\rangle_A \xrightarrow{U_E} |E_2\rangle_E |t'_2\rangle_P,$$

with orthogonal $|E_1\rangle, |E_2\rangle$. Readers might notice that this attack is similar to “faked states” attacks [19, 20] described in Section 3.2.3; we explore the connection between the two in Section 8.

While the above attack never causes an error, it increases the loss rate—Bob always gets a loss when using the Hadamard basis. This means that only bits encoded using the computational basis are used for transferring information, and Eve can copy the information, thus the scheme is insecure. We can compose another attack that does not have the property of causing a loss-rate 1 in a specific basis. For instance, by letting $p > 0$ Eve does not force a loss in the Hadamard basis, yet she does not learn the information for that basis.

⁸We limit the analysis to pulses that contain at most a single photon. Under this assumption, there are no invalid states for this setting.

C Interferometric BB84 With Added Measurements

In this subsection, we revisit the attack on the interferometric BB84 implementation from Appendix B. Recall that a Reversed-Space Attack stems from Eve being able to use time modes other than t'_0 and t'_1 in order to fool Bob's detection device.

However, by doing so, Eve creates pulses at times t_3 and t_{-1} at Bob's device, while such modes can never happen if only the incoming qubits arrive in time mode t'_0 and t'_1 , as they should be.

Therefore, let us consider a defense mechanism against the Reversed-Space Attack presented in Appendix B. Bob will measure both arms at times t_{-1} and t_3 in addition to the other six modes he measured before. Any pulse coming in any of these new modes will be interpreted by Bob as an invalid result.

We can now use the Reversed-Space formalism to analyze this new implementation, define the enlarged space that Eve can use (note, this space will be different from the one in Appendix B due to the added measurements), and check if Reversed-Space Attacks still exist in this new setting.

We constrain ourselves in the following ways: (i) Eve can only send zero or one photons; (ii) Eve attacks each pulse separately; and (iii) the optical components of Bob's device are perfectly implemented.

C.1 Bob's Measured Space

As stated, Bob will now measure pulses arriving at times t_{-1} and t_3 . Thus, his measured space is:

$$\mathcal{H}^B = \text{span} \{ |V\rangle, |s_{-1}\rangle, |d_{-1}\rangle, |d_0\rangle, |d_0\rangle, |s_1\rangle, |d_1\rangle, |s_2\rangle, |d_2\rangle, |s_3\rangle, |d_3\rangle \}. \quad (29)$$

Bob's unitary is the same for both measurement bases, and is identical to the one given in Section 5.3 ($\phi = 0$ still holds):

$$U_B |t'_i\rangle = (|s_t\rangle + i|d_t\rangle - |s_{t+1}\rangle + i|d_{t+1}\rangle) / 2. \quad (30)$$

Bob's interpretation sets for the computational basis are given by:

$$\begin{aligned} J_0 &= \{ |s_0\rangle, |d_0\rangle \}, \\ J_1 &= \{ |s_2\rangle, |d_2\rangle \}, \\ J_{\text{loss}} &= \{ |d_1\rangle, |s_1\rangle \}, \\ J_{\text{invalid}} &= \{ |s_{-1}\rangle, |d_{-1}\rangle, |s_3\rangle, |d_3\rangle \}. \end{aligned} \quad (31)$$

Bob's interpretation sets for the Hadamard basis are given by:

$$\begin{aligned} J_0 &= \{ |d_1\rangle \}, \\ J_1 &= \{ |s_1\rangle \}, \\ J_{\text{loss}} &= \{ |s_0\rangle, |d_0\rangle, |s_2\rangle, |d_2\rangle \}, \\ J_{\text{invalid}} &= \{ |s_{-1}\rangle, |d_{-1}\rangle, |s_3\rangle, |d_3\rangle \}. \end{aligned} \quad (32)$$

C.2 Eve's Attack

As shown in Appendix B, each of Bob's measured space is affected by its respective time bin at the entrance to his apparatus, as well as the one preceding it. From this argument, the reversed space is given by:

$$\mathcal{H}^P = \text{span} \{ |t'_{-2}\rangle, |t'_{-1}\rangle |t'_0\rangle, |t'_1\rangle, |t'_2\rangle, |t'_3\rangle \}. \quad (33)$$

- For $|j\rangle = |s_{-1}\rangle$:

$$\epsilon_{1,-2}|E_{1,-2}\rangle - \epsilon_{1,-2}|E_{1,-2}\rangle = 0. \quad (43)$$

- For $|j\rangle = |s_0\rangle$:

$$\begin{aligned} \epsilon_{1,-1}|E_{1,-1}\rangle - \epsilon_{1,0}|E_{1,0}\rangle &= 0 \\ \Downarrow \\ \epsilon_{1,-2} &= \epsilon_{1,-1} = \epsilon_{1,0}. \end{aligned} \quad (44)$$

- For $|j\rangle = |s_3\rangle$:

$$\epsilon_{1,2}|E_{1,2}\rangle - \epsilon_{1,3}|E_{1,3}\rangle = 0. \quad (45)$$

- For $|j\rangle = |d_{-1}\rangle$:

$$\begin{aligned} \epsilon_{1,-2}|E_{1,-2}\rangle + \epsilon_{1,-2}|E_{1,-2}\rangle &= 0 \\ \Downarrow \\ \epsilon_{1,-2} &= \epsilon_{1,-1} = \epsilon_{1,0} = 0. \end{aligned} \quad (46)$$

- For $|j\rangle = |d_0\rangle$:

$$\epsilon_{1,-1}|E_{1,-1}\rangle + \epsilon_{1,0}|E_{1,0}\rangle = 0. \quad (47)$$

$\underset{=0}{\epsilon_{1,-1}} \quad \quad \quad \underset{=0}{\epsilon_{1,0}}$

- For $|j\rangle = |d_3\rangle$:

$$\begin{aligned} \epsilon_{1,2}|E_{1,2}\rangle + \epsilon_{1,3}|E_{1,3}\rangle &= 0 \\ \Downarrow \\ \epsilon_{1,2} &= \epsilon_{1,3} = 0. \end{aligned} \quad (48)$$

From Eqs. (36)–(48), we notice that the only non-zero coefficients left are $\epsilon_{0,0}$ and $\epsilon_{1,1}$. Thus, our attack must satisfy:

$$\begin{aligned} U_E|0\rangle_E|t'_0\rangle_A &= \epsilon_{0,0}|E_{0,0}\rangle_E|t'_0\rangle, \\ U_E|0\rangle_E|t'_1\rangle_A &= \epsilon_{1,1}|E_{1,1}\rangle_E|t'_1\rangle. \end{aligned} \quad (49)$$

Hadamard Basis Let us consider $|\psi\rangle_A = |+\rangle = \frac{1}{\sqrt{2}}(|t'_0\rangle + |t'_1\rangle)$. We must avoid the states:

$$J_{\text{error}} = J_1 \cup J_{\text{invalid}} = \{|s_{-1}\rangle, |d_{-1}\rangle, |s_1\rangle, |s_3\rangle, |d_3\rangle\}. \quad (50)$$

For $|j\rangle = |s_1\rangle$, we get:

$$\begin{aligned} \sum_k \epsilon_{0,k} \beta_{k,d_1} |E_{0,k}\rangle + \sum_k \epsilon_{1,k} \beta_{k,d_1} |E_{1,k}\rangle &= 0 \\ \Downarrow \\ \frac{i}{\sqrt{2}}(-\epsilon_{0,0}|E_{0,0}\rangle + \epsilon_{0,1}|E_{0,1}\rangle) + \frac{i}{\sqrt{2}}(-\epsilon_{1,0}|E_{1,0}\rangle + \epsilon_{1,1}|E_{1,1}\rangle) &= 0 \\ \Downarrow \\ \epsilon_{0,0}|E_{0,0}\rangle &= \epsilon_{1,1}|E_{1,1}\rangle. \end{aligned} \quad (51)$$

$\underset{=0}{\epsilon_{0,0}} \quad \quad \quad \underset{=0}{\epsilon_{1,1}}$

Applying the result of Eq. (51) to Eq. (49), we get that the only attack Eve can apply without introducing noise is the trivial attack:

$$\begin{aligned} U_E|0\rangle_E|0\rangle_A &= |\phi\rangle_E|0\rangle_A, \\ U_E|0\rangle_E|1\rangle_A &= |\phi\rangle_E|1\rangle_A \\ \Downarrow \\ U_E|0\rangle_E|\psi\rangle_A &= |\phi\rangle_E|\psi\rangle_A. \end{aligned} \quad (52)$$

Which is completely independent of Alice's input state. Applying the additional constraints derived from the Hadamard basis is unnecessary at this point.

We have shown there is no attack that satisfies the requirements defined at the start of the subsection (single-photon states, each input state attacked separately, no added vulnerabilities, zero added noise) and gains information on the shared key. \square

D Additional Examples for Reversed-Space Attacks

In this appendix, we give additional examples for the application of the ideas from Section 5 on different setups, especially on the computation of the classical interpretation J sets and the process of finding an oblivious attack.

D.1 Examples of Interpretation Sets in Imperfect Bob Setups

Recall the example of measurement imperfections in Section 3.2.1 where Bob receives a pulse of photons with uniform polarization, written as the Fock space state $|m_1, m_0\rangle^F$ with $m_1, m_0 \geq 0$. Let us assume that Bob's detector cannot distinguish one photon from two or more photons, i.e., any state $|0, k\rangle^F$ with $k \geq 1$ causes the "0" detector to click, while any state $|k, 0\rangle^F$ with $k \geq 1$ causes the "1" detector to click. To make the analysis easier, we limit the discussion below to pulses with at most two photons.

In a BB84 implementation using this setting, Bob chooses to either measure using the computational basis (rectilinear polarization) or the Hadamard basis (diagonal polarization). We denote these settings by $s = 1$ and $s = 2$, respectively. To measure in the computational basis, Bob simply lets the state go into his detector; to measure in the Hadamard basis, Bob applies the Hadamard gate on the pulse and then measures the outcome.

The Hadamard gate evolves the possible 6 states (i.e., pulses with up to 2 photons) as

$$\begin{aligned} (1) \quad |0, 0\rangle^F &\rightarrow |0, 0\rangle^F & (4) \quad |1, 1\rangle^F &\rightarrow (|0, 2\rangle^F - |2, 0\rangle^F)/\sqrt{2} \\ (2) \quad |0, 1\rangle^F &\rightarrow (|0, 1\rangle^F + |1, 0\rangle^F)/\sqrt{2} & (5) \quad |0, 2\rangle^F &\rightarrow (|0, 2\rangle^F + \sqrt{2}|1, 1\rangle^F + |2, 0\rangle^F)/2 \\ (3) \quad |1, 0\rangle^F &\rightarrow (|0, 1\rangle^F - |1, 0\rangle^F)/\sqrt{2} & (6) \quad |2, 0\rangle^F &\rightarrow (|0, 2\rangle^F - \sqrt{2}|1, 1\rangle^F + |2, 0\rangle^F)/2. \end{aligned}$$

Using the same numbering for basis state, for the $s = 1$ setting we have $\beta_{[1,6] \times [1,6]}^{s=1} = I$, and for the $s = 2$ setting,

$$\beta_{[1,6] \times [1,6]}^{s=2} = \begin{pmatrix} 1 & 0 & 0 & 0 & 0 & 0 \\ 0 & 1/\sqrt{2} & 1/\sqrt{2} & 0 & 0 & 0 \\ 0 & 1/\sqrt{2} & -1/\sqrt{2} & 0 & 0 & 0 \\ 0 & 0 & 0 & 0 & 1/\sqrt{2} & -1/\sqrt{2} \\ 0 & 0 & 0 & 1/\sqrt{2} & 1/2 & 1/2 \\ 0 & 0 & 0 & -1/\sqrt{2} & 1/2 & 1/2 \end{pmatrix}.$$

We can assume that Bob considers the case where both detectors click as an invalid state, yet if no detector clicks, Bob considers this case as a valid loss. Then, using the notations presented in Section 5.2, $J_{\text{loss}} = \{|0, 0\rangle^F\}$ and $J_{\text{invalid}} = \{|1, 1\rangle^F\}$. The set J_{error} depends on the qubit sent by Alice. If Alice sends a 0 (either using the computational or the Hadamard basis) then a click of the "1"-detector is an error, and since the detector does not distinguish two photons from one we have $J_{\text{error}} = J_1 = \{|1, 0\rangle^F, |2, 0\rangle^F\}$. Similarly, if Alice sends a 1 then $J_{\text{error}} = J_0 = \{|0, 1\rangle^F, |0, 2\rangle^F\}$.

Bob adds no ancilla in this case, and his entire measured space arrives from the channel. Thus, from the reversed space analysis we get $\mathcal{H}^B = \mathcal{H}^P$. Note that the reversed space in this case has a larger dimension than the theoretical qubit space sent by Alice: it also includes pulses with zero photons and pulses with two photons.

If we do not limit ourselves to attacks in which Eve sends at most two photons, we can recover a well known attack: for this, we need to add the assumption that if both Bob's detectors click, he considers this invalid outcome as a loss and ignores it. In this case, Eve can perform a measure-and-resend attack in one of the bases, such that when she resends, the state is the same as the one she measured, but with a much larger number of photons (this is an example of the "faked states" [19, 20] attacks described in Section 3.2.3). For example, if Eve measures

$|0, 1\rangle^F$, she sends $|0, m\rangle^F$ with $m \gg 1$. Given that Bob's detector do not distinguish one photon from many, if Bob uses the same basis as Eve, he gets a legitimate result, and he never gets errors; and if he measures in the other basis, many photons enter both detectors (with high probability), both detectors click, and Bob ignores this outcome. This attack allows Eve to get full information without being noticed [55, 60].

D.2 Insecurity of Interferometric BB84: When Bob Does Not Measure All Modes

Consider the case in which Bob wants to open his detector only during a single detection slot. This may be done in order to achieve a higher bit-rate, or may be forced due to technological (or financial) limitations that restrict Bob from opening the detectors to more than a single detection window per pulse.⁹ A possible scheme for such a limited Bob is to measure only a single time-bin in each detector. For instance, to perform a measurement in the computational basis, assume Bob measures only $\{|d_0\rangle, |s_2\rangle\}$, i.e., opening the d -arm detector at time t_0 (to measure $|0\rangle$) and the s arm detector at time t_2 (to measure $|1\rangle$). For measuring in the Hadamard basis, Bob opens both his detectors at time t_1 : that is, he measures $|d_1\rangle, |s_1\rangle$ to indicate $|+\rangle$ and $|-\rangle$, respectively. This (practical) weakening of Bob leads to a stronger attack in which the detection efficiency in each basis is reduced by half; yet, in contrast to the attack described in Section 5.3 and Appendix B, it is not the case where one basis will always yield a loss.

Using the tools presented in Section 5.2, we find \mathbf{U}_{zero} (defined in Definition 7 as the set of attacks not causing any error) and discover that it includes attacks capable of revealing the information in its entirety to Eve. It should be noted that, as in Appendix B, the attacks are individual-particle attacks in which Eve uses only single-photon pulses; limiting Eve to single-photon pulses simplifies the analysis and is sufficient for proving insecurity.

Note that a basis of \mathcal{H}^B in this restricted case is defined as $B = \{|V\rangle, |d_0\rangle, |d_1\rangle, |s_1\rangle, |s_2\rangle\}$. The reversed space \mathcal{H}^P in this case (following Eq. (23) and Section B.2) is the span of $\{|V\rangle, |t'_{-1}\rangle, |t'_0\rangle, |t'_1\rangle, |t'_2\rangle\}$.

Bob interprets his measurement outcome in the following manner: for the Hadamard basis, $J_0 = \{|d_1\rangle\}$; $J_1 = \{|s_1\rangle\}$; $J_{\text{loss}} = B \setminus (J_0 \cup J_1)$; and $J_{\text{invalid}} = \emptyset$. For the computational basis, Bob uses the following interpretation: $J_0 = \{|d_0\rangle\}$; $J_1 = \{|s_2\rangle\}$; $J_{\text{loss}} = B \setminus (J_0 \cup J_1)$; the set J_{invalid} is empty again due to the assumption of using only single-photon pulses.

As done in Appendix B, we use Observation 1 to define the set of Eve's attacks that cause no errors. The requirements for the Hadamard basis are the same as in Section B.3 and are given by Eqs. (24)–(25). The requirements for the computational basis are

$$\epsilon_{t'_0, t'_1} |E_{t'_0, t'_1}\rangle - \epsilon_{t'_0, t'_2} |E_{t'_0, t'_2}\rangle = 0 \quad \text{when Alice sends } |0\rangle, \text{ and} \quad (53)$$

$$i\epsilon_{t'_1, t'_{-1}} |E_{t'_1, t'_{-1}}\rangle + i\epsilon_{t'_1, t'_0} |E_{t'_1, t'_0}\rangle = 0 \quad \text{when Alice sends } |1\rangle. \quad (54)$$

Thus, the family of Eve's attacks that cause no errors is of the form (omitting the vacuum state)

$$\begin{aligned} |0\rangle_E |0\rangle_A &\xrightarrow{U_E} p_1 |E_1\rangle_E |t'_{-1}\rangle_P + p_2 |E_2\rangle_E |t'_0\rangle_P + p_3 |E_3\rangle_E |t'_1\rangle_P + p_3 |E_3\rangle_E |t'_2\rangle_P \\ |0\rangle_E |1\rangle_A &\xrightarrow{U_E} -p_3 |E_3\rangle_E |t'_{-1}\rangle_P + p_3 |E_3\rangle_E |t'_0\rangle_P + p_2 |E_2\rangle_E |t'_1\rangle_P + p_4 |E_4\rangle_E |t'_2\rangle_P, \end{aligned}$$

with the normalization conditions $|p_1|^2 + |p_2|^2 + 2|p_3|^2 = |p_4|^2 + |p_2|^2 + 2|p_3|^2 = 1$.

It follows that Alice's qubit evolves as

$$\begin{aligned} |0\rangle_A \rightarrow & \frac{p_1 |E_1\rangle}{2} |s_{-1}\rangle + \frac{p_2 |E_2\rangle - p_1 |E_1\rangle}{2} |s_0\rangle + \frac{p_3 |E_3\rangle - p_2 |E_2\rangle}{2} |s_1\rangle + \frac{p_3 |E_3\rangle}{2} |s_3\rangle + i \frac{p_1 |E_1\rangle}{2} |d_{-1}\rangle \\ & + i \frac{p_2 |E_2\rangle + p_1 |E_1\rangle}{2} |d_0\rangle + i \frac{p_3 |E_3\rangle + p_2 |E_2\rangle}{2} |d_1\rangle + 2i \frac{p_3 |E_3\rangle}{2} |d_2\rangle + i \frac{p_3 |E_3\rangle}{2} |d_3\rangle \end{aligned}$$

⁹This issue is usually relevant in telecommunication wave length (IR spectrum) technology.

$$\begin{aligned}
|1\rangle_A \rightarrow & \frac{-p_3|E_3\rangle}{2}|s_{-1}\rangle + 2\frac{p_3|E_3\rangle}{2}|s_0\rangle + \frac{p_2|E_2\rangle - p_3|E_3\rangle}{2}|s_1\rangle + \frac{p_4|E_4\rangle - p_2|E_2\rangle}{2}|s_2\rangle - \frac{p_4|E_4\rangle}{2}|s_3\rangle \\
& + i\frac{p_3|E_3\rangle}{2}|d_{-1}\rangle + i\frac{p_2|E_2\rangle + p_3|E_3\rangle}{2}|d_1\rangle + i\frac{p_2|E_2\rangle + p_4|E_4\rangle}{2}|d_2\rangle + i\frac{p_4|E_4\rangle}{2}|d_3\rangle,
\end{aligned}$$

and never causes an error in the computational basis. For the Hadamard basis, $|+\rangle_A$ and $|-\rangle_A$ follow from the above by linearity. For concreteness, we only note that the projection on the states Bob measure behaves as required, i.e.,

$$\begin{aligned}
|+\rangle_A & \rightarrow 0 \cdot |s_1\rangle + \frac{i(p_3|E_3\rangle + p_2|E_2\rangle)}{\sqrt{2}}|d_1\rangle + \dots \\
|-\rangle_A & \rightarrow \frac{p_3|E_3\rangle - p_2|E_2\rangle}{\sqrt{2}}|s_1\rangle + 0 \cdot |d_1\rangle + \dots
\end{aligned}$$

Let us define the variable r as the bit value measured by Bob (restricted to the case where Bob and Alice use the same basis, and no loss has occurred). When Bob's outcome is r , Eve holds a state as described in Table 1.

Alice's State	Eve's State / $r = 0$	Eve's State / $r = 1$
$ 0\rangle_A$	$p_1 E_1\rangle_E + p_2 E_2\rangle_E$	—
$ 1\rangle_A$	—	$p_4 E_4\rangle_E - p_2 E_2\rangle_E$
$ +\rangle_A$	$p_3 E_3\rangle_E + p_2 E_2\rangle_E$	—
$ -\rangle_A$	—	$p_3 E_3\rangle_E - p_2 E_2\rangle_E$

Table 1: The non-normalized states Eve holds as a function of the state sent by Alice, conditioned on Bob measuring the bit value r (and not a loss)

Eve can acquire full information about the original state, for instance, by setting $p_i = 1/2$, $|E_1\rangle = |E_4\rangle$, and letting $|E_i\rangle_E$ be orthogonal for $i = 1, 2, 3$. Once Alice reveals the basis used, Eve measures her state and reveals Alice's bit with certainty. However, this reduces Bob's detection efficiency: when no attack is present, Bob measures a valid value with probability $1/2$ for the computational basis, and probability $1/2$ for the Hadamard basis. With the above attack, Bob's detection efficiency decreases to $1/8$ in the computational basis and $1/4$ in the Hadamard basis. By setting the parameters $\{p_i\}_{i=1,2,3,4}$, Eve can consider a tradeoff between the amount of information she acquires and the loss rate she induces on Bob.

E Formal Definition of Quantum Side-Channel Attacks

This is the formal formulation of Definition 8, presented in Section 6.

- Let $\mathcal{H}_{\text{full}}^A$ be the Hilbert space of all states that can arrive from Alice's channel, and let $\mathcal{H}_{\text{full}}^B$ be the Hilbert space of all states that can arrive at Bob's channel.
- Let $\mathcal{H}^A \subseteq \mathcal{H}_{\text{full}}^A$ be the span of Alice's sent states, and let $\mathcal{H}^B \subseteq \mathcal{H}_{\text{full}}^B$ be the space of states that affect Bob's measurement¹⁰.
- Let \mathcal{H}^{env} be the Hilbert space representing the publicly available environment that is not part of the previously defined spaces.
- Let Eve's attack be defined as the following unitary transformation:

$$U_E : \mathcal{H}_{\text{full}}^A \otimes \mathcal{H}_{\text{in}}^{\text{anc}} \otimes \mathcal{H}^{\text{env}} \rightarrow \mathcal{H}_{\text{full}}^B \otimes \mathcal{H}_{\text{out}}^{\text{anc}} \otimes \mathcal{H}^{\text{env}},$$

where $\mathcal{H}_{\text{in}}^{\text{anc}}, \mathcal{H}_{\text{out}}^{\text{anc}}$ are Eve's private ancilla spaces.

¹⁰Note that in Section 5, this space is denoted by \mathcal{H}^P .

Definition 9. *Eve’s attack is a Quantum Side-Channel Attack if either of these two conditions is true:*

1. *Eve’s attack depends non-trivially on \mathcal{H}^{env} ,*
2. *or the output of Eve’s attack non-trivially affects either $\mathcal{H}_{\text{full}}^{\text{B}} \setminus \mathcal{H}^{\text{B}}$ or \mathcal{H}^{env} .*

F Computation of Bright Illumination Attack Using Reversed-Space

In this appendix, we show the full computation of the Reversed-Space Attack shown in Section 7.4, beginning from the behavior of the implementation that was discovered through Quantum Fuzzing in Section 7.3 and resulting in the original attack described in Section 7.1. Our modeling of the device will rely *only* on the information learned on the device from fuzzing, and on the fact that the device employs a single unitary transformation independently of the basis it wishes to measure.

Bob’s Measured Space

The vulnerabilities shown in Section 7.3 show that Bob’s device has an unintended configuration that can be triggered by Eve (the linear mode of the APDs), and that in this configuration, his device suffers from a collection of Measurement Space Vulnerabilities and Interpretation Vulnerabilities (defined in Section 3.2.1). We will now formally describe these vulnerabilities.

For a polarization-based BB84 state $|\psi\rangle$, let us use $|\psi\rangle^{\text{bright}}$ to denote the high-photon-number state of the same polarization.

Let us denote Bob’s unitary transformation on the input as U_{B} . Note that there is only one transformation U_{B} (that is, $m = 1$, in the notation of Section 5.2.2), because Bob uses a passive basis choice.

We denote the input states *after* the application of U_{B} in the following way:

$$\begin{aligned} |\psi_0\rangle_{\text{B}} &\triangleq U_{\text{B}}|0\rangle^{\text{bright}}, & |\psi_1\rangle_{\text{B}} &\triangleq U_{\text{B}}|1\rangle^{\text{bright}}, \\ |\psi_2\rangle_{\text{B}} &\triangleq U_{\text{B}}|+\rangle^{\text{bright}}, & |\psi_3\rangle_{\text{B}} &\triangleq U_{\text{B}}|-\rangle^{\text{bright}}. \end{aligned} \quad (55)$$

Note that, according to the definition of high-photon-number states with diagonal polarization, the overlap between “bright Hadamard” states and “bright computational” states is given, without loss of generality, by:

$$\langle +|^{\text{bright}}|0\rangle^{\text{bright}} = \left(\frac{1}{\sqrt{2^k}} \sum_{l=0}^k \sqrt{\binom{k}{l}} \langle l, k-l |_{\text{H,V}} \right) |0, k\rangle_{\text{H,V}} = \frac{1}{\sqrt{2^k}} = O\left(2^{-\frac{k}{2}}\right). \quad (56)$$

Thus, if the photon number k is high enough, we can approximate

$$|0\rangle^{\text{bright}}, |1\rangle^{\text{bright}} \in \text{span} \left\{ |+\rangle^{\text{bright}}, |-\rangle^{\text{bright}} \right\}^{\perp}.$$

and vice versa.

Therefore, the set $\{|0\rangle^{\text{bright}}, |1\rangle^{\text{bright}}, |+\rangle^{\text{bright}}, |-\rangle^{\text{bright}}\}$ is orthonormal, and since U_{B} is unitary, so is the set $\{|\psi_0\rangle_{\text{B}}, |\psi_1\rangle_{\text{B}}, |\psi_2\rangle_{\text{B}}, |\psi_3\rangle_{\text{B}}\}$. We thus model the Hilbert space that Bob measures as:

$$\mathcal{H}^{\text{B}} = \text{span} \{|\psi_0\rangle_{\text{B}}, |\psi_1\rangle_{\text{B}}, |\psi_2\rangle_{\text{B}}, |\psi_3\rangle_{\text{B}}\}. \quad (57)$$

Note that, since this is a BB84 implementation with passive basis choice, Bob’s choice of basis is performed by the device itself. From the Quantum Fuzzing procedure, we know Bob’s measurement interpretations (as defined in Section 5.2.3) in both bases:

- In the computational basis:

$$J_0 = \{|\psi_0\rangle_B\}, \quad J_1 = \{|\psi_1\rangle_B\}. \quad (58)$$

Since the states $|\psi_2\rangle_B$ and $|\psi_3\rangle_B$ always cause a Hadamard basis measurement, they can never be interpreted as part of a computational basis measurement, and can be omitted from consideration in this basis.

- In the Hadamard basis:

$$J_0 = \{|\psi_2\rangle_B\}, \quad J_1 = \{|\psi_3\rangle_B\}. \quad (59)$$

Similarly, since the states $|\psi_0\rangle_B$ and $|\psi_1\rangle_B$ always cause a computational basis measurement, they can never be interpreted as part of a Hadamard basis measurement, and can be omitted from consideration in this basis.

Eve's Attack

When reversing the space that Bob measures through Bob's unitary, we unsurprisingly get the space spanned by the four states we found by Quantum Fuzzing:

$$\mathcal{H}^P = \text{span} \left\{ U_B^\dagger |\psi_i\rangle_B \mid i = 0, 1, 2, 3 \right\} = \text{span} \left\{ |0\rangle^{\text{bright}}, |1\rangle^{\text{bright}}, |+\rangle^{\text{bright}}, |-\rangle^{\text{bright}} \right\}. \quad (60)$$

Thus, Eve's general form of attack is:

$$\begin{aligned} U_E |0\rangle_E |0\rangle_A &= \epsilon_{0,0} |E_{0,0}\rangle |0\rangle^{\text{bright}} + \epsilon_{0,1} |E_{0,1}\rangle |1\rangle^{\text{bright}} + \\ &\quad \epsilon_{0,2} |E_{0,2}\rangle |+\rangle^{\text{bright}} + \epsilon_{0,3} |E_{0,3}\rangle |-\rangle^{\text{bright}}, \\ U_E |0\rangle_E |1\rangle_A &= \epsilon_{1,0} |E_{1,0}\rangle |0\rangle^{\text{bright}} + \epsilon_{1,1} |E_{1,1}\rangle |1\rangle^{\text{bright}} + \\ &\quad \epsilon_{1,2} |E_{1,2}\rangle |+\rangle^{\text{bright}} + \epsilon_{1,3} |E_{1,3}\rangle |-\rangle^{\text{bright}}. \end{aligned} \quad (61)$$

Attack Constraints

The constraints, as defined in Section 5.2.3, are:

$$\begin{aligned} \forall |\psi\rangle_A = \sum_i \alpha_i |i\rangle_A, \quad \forall |j\rangle \in J_{\text{error}} : \\ \sum_{i,k} \alpha_i \epsilon_{i,k} \beta_{k,j} |E_{i,k}\rangle = 0, \end{aligned} \quad (62)$$

where $U_B = \sum_{k,j} \beta_{k,j} |j\rangle\langle k|$ is Bob's unitary transformation, together with orthonormality conditions on Eve's output states.

In this case, Bob's transformation is defined as $\beta_{k,j} = \delta_{k,j}$ (Kronecker delta). Therefore, the condition for our attack is: $\sum_{i,k} \alpha_i \epsilon_{i,k} \delta_{k,j} |E_{i,k}\rangle = 0$, which is easily simplified to:

$$\sum_i \alpha_i \epsilon_{i,j} |E_{i,j}\rangle = 0, \quad (63)$$

for all $|j\rangle \in J_{\text{error}}$. Let us apply the constraints to each measurement basis and each input state separately.

Computational Basis

- For $|0\rangle_A$: $\vec{\alpha} = (1, 0)$.

$$\forall |j\rangle \in J_{\text{error}} : \epsilon_{0,j}|E_{0,j}\rangle = 0.$$

Since $J_{\text{error}} = J_1 = \{|\psi_1\rangle_B\}$:

$$\epsilon_{0,1}|E_{0,1}\rangle = 0. \quad (64)$$

- For $|1\rangle_A$: $\vec{\alpha} = (0, 1)$.

$$\forall |j\rangle \in J_{\text{error}} : \epsilon_{1,j}|E_{1,j}\rangle = 0.$$

Since $J_{\text{error}} = J_0 = \{|\psi_0\rangle_B\}$:

$$\epsilon_{1,0}|E_{1,0}\rangle = 0. \quad (65)$$

Hadamard Basis

- For $|+\rangle_A$: $\vec{\alpha} = \left(\frac{1}{\sqrt{2}}, \frac{1}{\sqrt{2}}\right)$.

$$\forall |j\rangle \in J_{\text{error}} : \epsilon_{0,j}|E_{0,j}\rangle + \epsilon_{1,j}|E_{1,j}\rangle = 0.$$

Since $J_{\text{error}} = J_1 = \{|\psi_3\rangle_B\}$, we get:

$$\epsilon_{0,3}|E_{0,3}\rangle + \epsilon_{1,3}|E_{1,3}\rangle = 0. \quad (66)$$

- For $|-\rangle_A$: $\vec{\alpha} = \left(\frac{1}{\sqrt{2}}, \frac{-1}{\sqrt{2}}\right)$.

$$\forall |j\rangle \in J_{\text{error}} : \epsilon_{0,j}|E_{0,j}\rangle - \epsilon_{1,j}|E_{1,j}\rangle = 0.$$

Since $J_{\text{error}} = J_0 = \{|\psi_2\rangle_B\}$, we get:

$$\epsilon_{0,2}|E_{0,2}\rangle - \epsilon_{1,2}|E_{1,2}\rangle = 0. \quad (67)$$

Combining Eqs. (64)–(67), our generic attack can be written as:

$$\begin{aligned} U_E|0\rangle_E|0\rangle_A &= \epsilon_{0,0}|E_{0,0}\rangle|0\rangle^{\text{bright}} + \epsilon_{0,2}|E_{0,2}\rangle|+\rangle^{\text{bright}} + \epsilon_{0,3}|E_{0,3}\rangle|-\rangle^{\text{bright}}, \\ U_E|0\rangle_E|1\rangle_A &= \epsilon_{1,1}|E_{1,1}\rangle|1\rangle^{\text{bright}} + \epsilon_{1,2}|E_{1,2}\rangle|+\rangle^{\text{bright}} + \epsilon_{1,3}|E_{1,3}\rangle|-\rangle^{\text{bright}}, \end{aligned} \quad (68)$$

with the constraints:

$$\begin{aligned} \epsilon_{0,2}|E_{0,2}\rangle - \epsilon_{1,2}|E_{1,2}\rangle &= 0, \\ \epsilon_{0,3}|E_{0,3}\rangle + \epsilon_{1,3}|E_{1,3}\rangle &= 0, \\ ||U_E|0\rangle_E|0\rangle_A||^2 &= 1, \\ ||U_E|0\rangle_E|1\rangle_A||^2 &= 1, \\ (U_E|0\rangle_E|0\rangle_A)^\dagger (U_E|0\rangle_E|1\rangle_A) &= 0. \end{aligned} \quad (69)$$

This can be algebraically reduced to the following form:

$$\begin{aligned} U_E|0\rangle_E|0\rangle_A &= p|E_0\rangle|0\rangle^{\text{bright}} + q|E_2\rangle|+\rangle^{\text{bright}} + q|E_3\rangle|-\rangle^{\text{bright}}, \\ U_E|0\rangle_E|1\rangle_A &= p|E_1\rangle|1\rangle^{\text{bright}} + q|E_2\rangle|+\rangle^{\text{bright}} - q|E_3\rangle|-\rangle^{\text{bright}}, \end{aligned} \quad (70)$$

where p and q are non-negative real numbers (because without loss of generality, phase can be incorporated into Eve's ancillary states), with the constraint:

$$p^2 + 2q^2 = 1. \quad (71)$$

This concludes our construction of the attack. \square

G Examples of Attacks on QKD

This appendix lists QKD attacks and attack families used in Section 8, as well as high-level details on each attack.

G.1 List of Individual Attacks

- **Large Pulse Attack** [17]

This attack is discussed in Section 6.3.

- **Photon-Number Splitting (PNS) Attack** [16, 48]

This attack is discussed in Section 2.5.1 of [30].

- **Injection-Locking Attack** [22].

This attack is discussed in Section 6.3 of our work. Additional details appear in Table 4.35 of [30].

- **Time-Shift Attack** [23]

This attack is applicable in QKD receivers that use different photo-detectors to detect different states, and the detection windows of the detectors are not identical. Eve selectively makes Alice’s signal arrive earlier or later than the original detection time, making only one detection result possible. This attack does not rely on Eve measuring Alice’s signal to generate an appropriate state to send to Bob, which makes it highly practical.

Further details can be found in Table 4.5 of [30].

- **Trojan Pony Attack** [55, 32]

This attack is initially defined in [55] as one built under a two-adversary model. In this model, an additional adversary named Fred is inside Bob’s lab, and can get classical information from Eve to affect Bob’s device in a limited way. Fred cannot communicate back to Eve. In this setup, Bob’s detector is not fully efficient, and Fred has control over when to fail Bob’s detector. When Fred knows that Eve and Bob chose mismatching bases, he drops Eve’s photon.

A special case of this attack, given in [55], is a detector which behaves identically for pulses with a single photon and those with a high number of photons, and Bob treats double-click events as losses. In their work, [32] show that their implementation of this attack can be built using Reversed-Space.

G.2 List of Attack Families

- **Bright Illumination Attacks** [21]

The pulsed variant of this attack is analyzed in Section 7. Different variants appear in tables 4.12-4.14 and 4.17-4.20 of [30].

- **Faked States Attacks** [19, 38, 20]

This is a general family of intercept-resend attacks where Eve sends malicious signals to Bob, which cause him to get a result of her choice. Details appear in Section 2.5.2.1 of [30].

- **Fixed Apparatus Attacks** [24]

These attacks are applicable against all QKD implementations where Bob’s choice of basis is not active — for example, when a beam splitter is used for replacing Bob’s true choice of basis.

In some cases of the Fixed-Apparatus attack, Bob’s passive choice alone performs an enlargement of \mathcal{H}^B which Eve can use to build a Reversed-Space Attack.

In its general case, this attack model also considers a situation where Eve gains access to Bob’s ancillary space and can manipulate Bob’s ancillary state. Using this power, Bob’s effective measured space is enlarged for Eve (to be $\mathcal{H}^B \otimes \mathcal{H}^{\text{anc}}$ instead of \mathcal{H}^B) and she can build a Reversed-Space Attack.

- **Trojan Horse Attacks** [84, 18]

Trojan Horse attacks send light pulses into Alice or Bob’s devices, and study secret aspects of their configuration from the back-scattered light. Details appear in Table 4.48 of [30]. These attacks are a general case of the Large Pulse attack, as defined by [17]. The Large Pulse attack specifically probes devices by sending a high-intensity light pulse at a specific window, whereas Trojan Horse attacks are relatively generic. Note that Lo and Chau defined a different notion of “Trojan Horse” attacks [91, 92], but it is rarely used.

- **Reversed-Space Attacks** [27, 28]

These attacks are discussed in Section 5.

- **Detector Efficiency Mismatch Attacks** [19, 38]

This attack utilizes a receiver that uses several detectors in order to measure the incoming states, and their sensitivities are not completely identical. Eve uses the non-overlapping parts of the windows and sends fake states that force a specific state/basis measurement. As such, it is a special case of the Faked-States attack family. Details appear in Table 4.5 of [30].